Gondwana Research 24 (2013) 330–348

Contents lists available at SciVerse ScienceDirect

Gondwana Research

journal homepage: www.elsevier.com/locate/gr

High-resolution stable isotope stratigraphy of the upper Cambrian and Ordovician in the Argentine Precordillera: Carbon isotope excursions and correlations

A.N. Sial [a,*], S. Peralta [b], C. Gaucher [c], A.J. Toselli [d], V.P. Ferreira [a], R. Frei [e], M.A. Parada [f], M.M. Pimentel [g], Natan Silva Pereira [a]

[a] NEG-LABISE, Department of Geology, Federal University of Pernambuco, P.O. Box 7852, Recife, PE, 50670-000, Brazil
[b] Instituto de Geología, Universidad Nacional de San Juan-CONICET, 5400, Argentina
[c] Departamento de Paleontologia, Facultad de Ciencias, Iguá, 4225, 11400 Montevideo, Uruguay
[d] Instituto Superior de Correlación Geológica (INSUGEO), Miguel Lillo 205, San Miguel de Tucuman 4000, Argentina
[e] Institute of Geography and Geology, Geology Section, University of Copenhagen, Øster Voldgade 10, DK-1350 Copenhagen, Denmark
[f] Departamento de Geología, Universidad de Chile, Santiago, Chile
[g] Institute of Geosciences, Federal University of Rio Grande do Sul, Porto Alegre, RS, 91509-900, Brazil

ARTICLE INFO

Article history:
Received 30 November 2011
Received in revised form 10 October 2012
Accepted 17 October 2012
Available online 29 November 2012

Handling Editor: J.G. Meert

Keywords:
Carbon-isotope excursions
Oxygen isotope geochemistry
Argentine Precordillera
Upper Cambrian
Ordovician

ABSTRACT

We report the occurrence of important carbon isotope excursions in early Paleozoic formations of the Eastern and Central Argentine Precordillera. The Steptoean positive isotope carbon excursion (SPICE) is known from North America, Kazakhstan, South China, Australia and South America, and the negative isotope carbon excursion (SNICE) has been described for the first time in South America. We report here the record of the SPICE and SNICE in a single section in the Eastern Precordillera. In the Central Precordillera, a minor middle Darriwilian positive carbon isotope excursion (MDICE) and a late Sandbian positive isotope carbon excursion, the GICE (~+3‰; *C. bicornis* biozone) are reported from two sections. One pre-GICE positive carbon-isotope excursion (Sandbian Sa1, *N. gracilis* biozone) in the Central Precordillera with a $\delta^{13}C$ peak of ~+2‰ is, perhaps, equivalent to the positive Spechts Ferry $\delta^{13}C$ excursion of North America. A positive $\delta^{13}C$ excursion (~6‰; *N. persculptus* biozone) recorded at the base of the late Hirnantian La Chilca Formation probably corresponds to HICE.

These carbon-isotope excursions resulted from more than one factor where paleoceanographic events probably played a major role: (a) sea-level fall and vigorous fluctuations in the Steptoean (SPICE), (b) sea-level rise in the Sunwaptan (SNICE), (c) important transgression in the Sandbian (pre-GICE and GICE), and (d) sea-level fall in the late Hirnantian (HICE). In the Darriwilian and Sandbian stages, organic burial has led to a large ^{12}C sequestration in the deep anoxic ocean with saline bottom water, recorded by the graptoliferous black shales of the Gualcamayo and Los Azules formations in Central Precordillera, helped the building of the MDICE and GICE anomalies.

$\delta^{18}O$ values for the Upper Cambrian carbonates are likely near-primary isotope signals that point to progressive cooling from the SPICE to the SNICE, whereas for Sandbian carbonates they suggest strong temperature fluctuations. The $\delta^{13}C$ peak of the GICE coincides with a cooler period with temperatures warming up towards the late Hirnantian to Rhuddanian.

The Upper Cambrian to the Middle Ordovician of the Precordillera recorded a decrease of seawater $^{87}Sr/^{86}Sr$ ratios in accordance to the global picture. This decrease probably reflects the influence of widespread volcanic activity from arc terranes in low-latitude settings along eastern margins of Laurentia and in the Argentine Precordillera in the Early to Middle Ordovician. Five carbonate samples (from San Juan, Gualcamayo and Los Azules formations) yielded εNd values that along seven already published values seem to plot along the Nd isotopic evolution trend of the Iapetus Ocean.

Together, the record of global Upper Cambrian and Ordovician carbon-isotope excursions in the Argentine Precordillera is a valuable proxy in refining Early Paleozoic stratigraphy, establishing of regional/global high-resolution correlations, and sea-level change history in South America.

1. Introduction

Oceanic $\delta^{13}C_{carb}$ fluctuations during the Paleozoic appear transitional between vigorous fluctuations observed in the Neoproterozoic (±10‰) and the increasingly stable Mesozoic to Cenozoic periods

* Corresponding author at: NEG-LABISE, Department of Geology, Federal University of Pernambuco, C.P. 7852, CEP 50670-000, Recife, PE, Brazil. Tel.: +55 81 2126 8243; fax: +55 81 2126 8242.
E-mail address: sial@ufpe.br (A.N. Sial).

1342-937X/$ – see front matter
http://dx.doi.org/10.1016/j.gr.2012.10.014

(Saltzman, 2005). The composite $\delta^{13}C_{carb}$ variation curve for the Paleozoic shows several positive excursions, some with peaks of about +7‰ (e.g. Kump et al., 1999; Saltzman, 2005), comparable in amplitude to Neoproterozoic peaks but shorter in duration. These positive excursions have been regarded as lacking associated negative excursions which are known only at the beginning and end of the Paleozoic (Knoll et al., 1996; Montañez et al., 2000; Saltzman, 2005). However, a Sunwaptan negative $\delta^{13}C_{carb}$ anomaly (−4‰) associated to the positive Steptoean excursion in the Argentine Precordillera, the global nature of which needs further confirmation, has been reported by Sial et al. (2008).

A composite high-resolution $\delta^{13}C$ curve for the Middle Cambrian to the Pennsylvanian in North America (Saltzman, 2005), reveals that large positive excursions were common during cool periods (e.g., Upper Ordovician–Silurian and Late Devonian–Early Mississipian). This author proposed that periods of stability in $\delta^{13}C$ reflect negative feedbacks on bioproductivity in a nitrogen-limited ocean where anoxia led to increased denitrification.

Ten Cambrian large-scale $\delta^{13}C$ excursions have been defined (Álvaro et al., 2008) from the BACE (Basal Cambrian Isotope Excursion) to the TOCE (Top of Cambrian Excursion). None of these biogeochemical events, however, have been directly related to glaciation; some have been associated to sea-level fall that may be eustatic in origin (Ripperdan, 2002). Additionally, it seems likely that these excursions are related to faunal turnover and diversification, as well as to the progressive increase in bioturbation and ventilation of organic-rich sediments through Cambrian time (Droser and Bottjer, 1988).

A large and global positive $\delta^{13}C$ excursion for Upper Cambrian (Steptoean) carbonates has been reported from North America, Kazakhstan, South China and Australia and marks the beginning of a global extinction of trilobites (Saltzman et al., 1998, 2000). This Steptoean positive C-isotope excursion (~+5‰), described by the acronym SPICE (Saltzman et al., 1998) represents a major perturbation of the Cambrian carbon cycle at ~500 Ma and, as a peculiarity, a worldwide mass extinction (mainly trilobites among other faunas) coincides with the onset of the positive shift, rather than with the rising limb of the excursion. The peak of faunal diversity correlates in North America with the peak of SPICE (Saltzman et al., 2000). The SPICE is believed to have had a duration of about 4 Myr (Saltzman et al., 1998), although 3 Myr is probably a better estimate, according to Peng and Babcock (2008). One interpretation of the SPICE ascribes it to increased burial of organic carbon, which is enriched in ^{12}C, thus increasing the ^{13}C pool in the oceans. However, terrestrial weathering impacts related to sea-level and/or climate change have also been considered as explanations (Saltzman et al., 2000, 2004; Gill et al., 2007).

C-isotope variation curves for the Cambrian–Ordovician boundary at Black Mountain, Australia (Ripperdan et al., 1992), and at Lawson Cove, Ibex area, Utah (Ripperdan and Miller, 1995), reveal a pronounced negative C-isotope excursion (−4‰) in the uppermost Cambrian (Sunwaptan Stage). The Cambrian–Ordovician boundary is characterized by synchronous changes in sea-level conodont (*Paltodus deltifer* in Precordillera) biozones, and $\delta^{13}C$ of marine carbonates (Ripperdan et al., 1992).

A Sunwaptan negative C-isotope excursion first observed in the Argentine Precordillera, in La Flecha Formation at Quebrada de la Flecha, has been named SNICE by Sial et al. (2008) and, if demonstrated to be a global event, combined with SPICE can be valuable tools for high-resolution correlation and can be used to locate primary subdivisions of the Cambrian system in unfossiliferous carbonate sequences globally.

In the Ordovician, three major carbon isotope excursions are known. Two of them have been recognized in the Upper Ordovician, one in the Early Chatfieldian North American Stage (Sandbian to early Katian), and another in the Gamachian Stage (Hirnantian) (Brenchley et al., 2003; Saltzman et al., 2003; Bergström et al., 2006; Kaljo et al., 2007 and references therein). The latter excursion is known as Hirnantian Isotope Carbon Excursion (HICE) (see Orth et al., 1986; Finney et al., 1999; Brenchley et al., 2003; Melchin et al., 2003; Fan et al., 2009; Jones et al., 2011) and the former as Guttenberg Isotope Carbon Excursion (GICE) also recorded in Sweden and Estonia, in Baltoscandia, and China (see Ainsaar et al., 1999; Brenchley et al., 2003; Saltzman et al., 2003; Saltzman and Young, 2005; Kaljo et al., 2007; Young et al., 2008; Ainsaar et al., 2010; Bergström et al., 2010).

The GICE anomaly was first recognized in the Guttenberg Member of the Decorah Formation in Iowa (Hatch et al., 1987; Ludvigson et al., 1996, 2000). According to Saltzman et al. (2003), in this region the GICE is expressed by a relatively abrupt change in $\delta^{13}C$ curve from −2‰ to −1‰ to about +2 to +3‰ followed upwards by a drop drown to previous values. It is not yet clear, according to them, if GICE starts in the uppermost part of the *C. americanus* Zone, or in the overlying *O. ruedmanni* Zone, but it does not appear to extend into the *C. spiniferus* Zone (see Fig. 1). In North American sections containing the widespread Millbrig K-bentonite, the base of the GICE starts in a transgressive interval above this ash bed (Bergström et al., 2010). This excursion ends in a regressive interval and its thickness varies from 1 m to over 100 m. Below the GICE interval, Ludvigson et al. (2004) have recognized four minor pre-GICE $\delta^{13}C$ positive excursions in North America, regarded as regional, namely in descending order: Spechts Ferry, Quimby's Mill, Grand Detour, and Mifflin, in the Turinian (early Sandbian).

According to Schmitz et al. (2010), the relationship between the GICE and potential climatic and water temperature indicators (lithofacies, faunas, and geochemistry) does not suggest a close correlation to specific environmental conditions. However, Saltzman and Young (2005) have interpreted this $\delta^{13}C$ excursion as a record of enhanced organic carbon burial, which lowered atmospheric pCO_2 to levels near the threshold for ice buildup in the Ordovician greenhouse climate.

Towards the end of the Hirnantian, cold temperature, major glaciation and severe drop in sea-level, were replaced by temperature rise, melting of glaciers and sea level return to the same level or slightly higher that it had been prior to glaciations (Munnecke et al., 2010). The Hirnantian mass extinction was the second largest extinction event in geologic time, according to these authors. HICE, the most prominent of the three major global $\delta^{13}C$ excursions in the Ordovician, has been recorded from the uppermost Ordovician in Nevada, Quebec, Arctic Canada, Baltoscandia, Scotland, China, and North American Midcontinent (Ripperdan et al., 1998; Finney et al., 1999; Bergström et al., 2006; Schmitz et al., 2010). HICE maximum peak values of up to +5‰ have been reported from North America, and up to +6‰ from Estonia and Latvia (e. g., Bergström et al., 2010; Brenchley et al., 2003).

There is a consensus that HICE is of global distribution and associated with a major glaciation (Bergström et al., 2006; Jones et al., 2011). It occupies a biostratigraphically well-defined interval in the graptolite and chitinozoan zone successions (Finney et al., 1999; Soufiane and Achab, 2000; Melchin et al., 2003; Kaljo et al., 2004; Melchin and Holmden, 2006). Sea-level change–HICE relationships in the Anticosti Island, Canada, indicate that they were not perfectly coupled (Jones et al., 2011), the start of the isotope excursion and the initial sea-level drawdown were coincident, but the excursion persisted through the deglacial sea-level rise and only reaching its peak after sea level had begun to rise.

The stratigraphically oldest of the named Ordovician $\delta^{13}C$ excursions, the Middle Ordovician (Darriwilian) $\delta^{13}C$ excursion (MDICE), is the least known among the three major Ordovician positive $\delta^{13}C$ excursions. This excursion is known from the Middle Ordovician of Baltoscandia and recently has been identified from the Guniutan Formation at two localities in the Yangtze platform, China (Schmitz et al., 2010). According to these authors, such occurrences in strata with striking lithological and conodont faunal similarity to the Swedish Holen Limestone and some coeval units in Estonia, suggest that MDICE likely has a worldwide distribution, with potential for local and long-range chemostratigraphic correlations.

In Fig. 1, the chrono-biostratigraphic chart for the Upper Cambrian and Ordovician is summarized showing the correlation between the

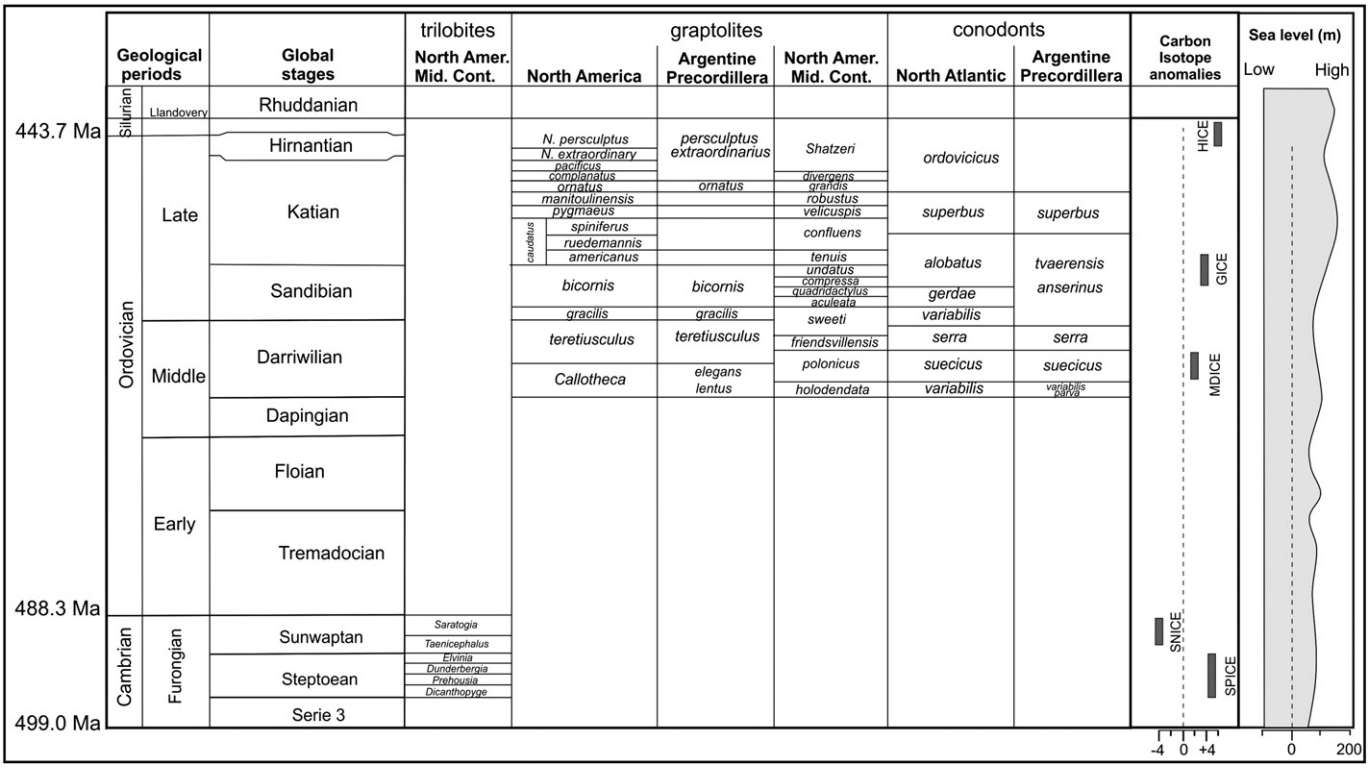

Fig. 1. Upper Cambrian and Ordovician stratigraphic correlation chart between the diagnostic graptolite, conodont zones and global Stage names used in this study (after Albanesi and Ortega, 2002; Young et al., 2008). Upper Cambrian trilobite zones are from Elrick et al. (2011). The relative sea-level curve is from Haq and Schutter (2008). Duration of positive carbon isotope excursions (SPICE, MDICE, GICE, HICE) have been compiled from several sources (Finney et al., 1999; Saltzman et al., 2003; Bergström et al., 2006; Sial et al., 2008; Bergström et al., 2010).

corresponding diagnostic trilobite, graptolite, and conodont biozones, including the Argentine Precodillera (after Albanesi and Ortega, 2002; Young et al., 2008; Elrick et al., 2011). The approximate duration of the main Upper Cambrian and Ordovician carbon isotope anomalies has been summarized from Finney et al. (1999), Saltzman et al. (2003), Bergström et al. (2006, 2010) and Sial et al. (2008) and the relative sea-level variation curve is from Haq and Schutter (2008).

Carbon-isotope studies on Upper Cambrian and Upper Cambrian–Lower Ordovician carbonates of the Argentine Precordillera were carried out by Ramos et al. (1999) and Buggisch et al. (2003), respectively. Sial et al. (2008) studied the carbon, oxygen and strontium-isotope chemostratigraphies of representative Upper Cambrian sections of the Eastern and Central Precordillera in San Juan Province, at their type localities (Quebrada de La Flecha, Cerro La Silla and Quebrada de Zonda) and at Quebrada de La Angostura in the northern part of the Central Precordillera. These authors reported the occurrence of the SPICE anomaly (+5‰) in the La Flecha Formation at Quebrada de La Angostura and of an important negative carbon-isotope excursion (−4‰) in this formation at Quebrada de La Flecha (SNICE).

In the present study, we sampled carbonates in order to identify the SPICE and SNICE in a single section in the Argentine Precordillera, and also for the three major Ordovician positive carbon-isotope anomalies (MDICE, GICE and HICE) whose occurrence in South America are still unknown. Relatively good preservation of Cambrian and Ordovician carbonate rocks in the Argentine Precordillera makes this region unique for chemostratigraphic and palaeoenvironment studies.

2. Studied Upper Cambrian–Ordovician sections

2.1. Geological setting

The Precordillera Geological Province which includes three morphological units (Eastern, Central and Western Precordillera; Ortiz and Zambrano, 1981; Baldis and Chebli, 1969; Baldis et al., 1982) is a typical thin-skinned thrust-and-fold belt, of about 600 km in length, exposed in northwestern Argentina.

Cambrian to Lower–Middle Ordovician platformal carbonate successions occur exclusively in the Eastern and Central Precordillera; in the western Precordillera they appear only as resedimented deposits (Bordonaro, 2003a,b). Whereas mixed and siliciclastic Upper Ordovician deposits are widely distributed in the Precordillera, Silurian to Lower Devonian siliciclastic deposits are important components only in the Eastern and Central Precordillera. The Cambrian to Devonian successions belong to the Famatinan tectonic cycle, from a tectono-sedimentary point of view (Aceñolaza and Toselli, 1999).

2.2. Eastern Precordillera: Quebrada Juan Pobre Section (Late Cambrian)

At the Quebrada de Juan Pobre section in the Sierra Chica de Zonda, Eastern Precordillera, La Laja (Juan Pobre Member) and Zonda formations occur (Figs. 2, 3, and 4a). While the former is mainly composed of limestones, in the latter limestones at the base pass into dolomitic limestones and dolostones upsection. In the Quebrada de Juan Pobre, the Zonda Formation has been supposedly deposited during the Steptoean according to Keller (1999). This unit, 350 m thick, is predominantly composed of dolomitic limestone (mudstone–boundstone) in its lower part (~110 m thick). Microbial dolostone and intraformational conglomerates in the upper part (~240 m thick) exhibit shallow-water sedimentary structures, such as mud-cracks, fenestral fabrics, bird eyes, flat-pebble conglomerate, cross-bedding, planar and domical stromatolites. In the succession, shallowing-upward cycles have been recognized by Arroqui Langer and Bordonaro (1996). Trilobites of the *Bolaspidella* zone occur at the base of the Zonda Formation (Bordonaro, 1990). The presence of *Plethopeltis* cf. *P. saratogensis* zone which occurs at the base of the overlying La Flecha Formation,

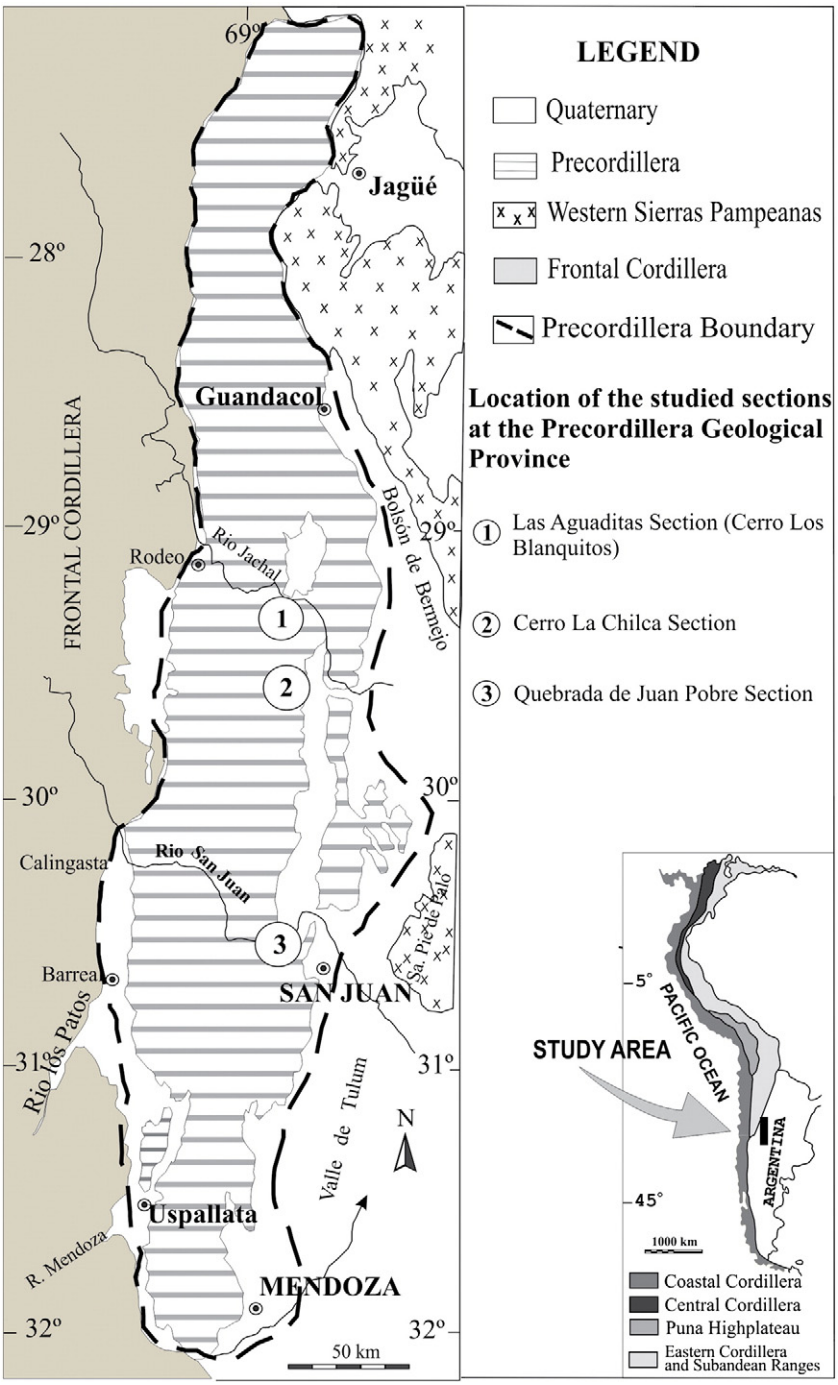

Fig. 2. Location map of the three studied sections in the Argentine Precordillera: Quebrada de Juan Pobre, Cerro La Chilca and Los Blanquitos ridge (Las Aguaditas section). Modified from Baldis et al. (1982).

indicating late Sunwaptan age (Vaccari, 1994), has not been reported so far in the Quebrada de Juan Pobre section.

2.3. Central Precordillera: Cerro La Chilca Section (Ordovician)

A thick lower Paleozoic succession crops out west of the Cerro La Chilca, Central Precordillera (Fig. 2). The Cerro La Chilca is occupied by an asymmetric anticlinal structure with Paleozoic rocks exposed on its western flank. On the eastern side of this ridge, a thrust fault striking N–S bounds the block and can be traced for over a hundred kilometers.

The Ordovician succession at the Cerro La Chilca consists, from base to top, of the following lithostratigraphic units (Fig. 3): San Juan (Tremadoc to Darriwillian; Mestre and Heredia, 2012), Gualcamayo (Darriwilian; Cuerda and Furque, 1985; Peralta, 1998), Los Azules (Sandbian; Blasco and Ramos, 1976; Cuerda and Furque, 1985; Peralta, 1998) and Don Braulio formations (late Hirnantian; Astini and Benedetto, 1992). These units are followed by the late Hirnantian to early Wenlockian La Chilca Formation (Cuerda et al., 1988), the Wenlockian–Ludlowian Los Espejos Formation (Cuerda, 1969), and the Lower Devonian Talacasto and Punta Negra formations (Peralta, 2003).

The San Juan Formation is fault-bounded at the base. At the top of this unit, a prominent hard-ground developed, characterized by vertical burrows that penetrate several centimeters into the uppermost bed of the unit. The San Juan Formation is a limestone-dominated succession with minor marls near the top. Dolostones occur as patches of brown to yellow microspar in connection with pressure solution or as burrow

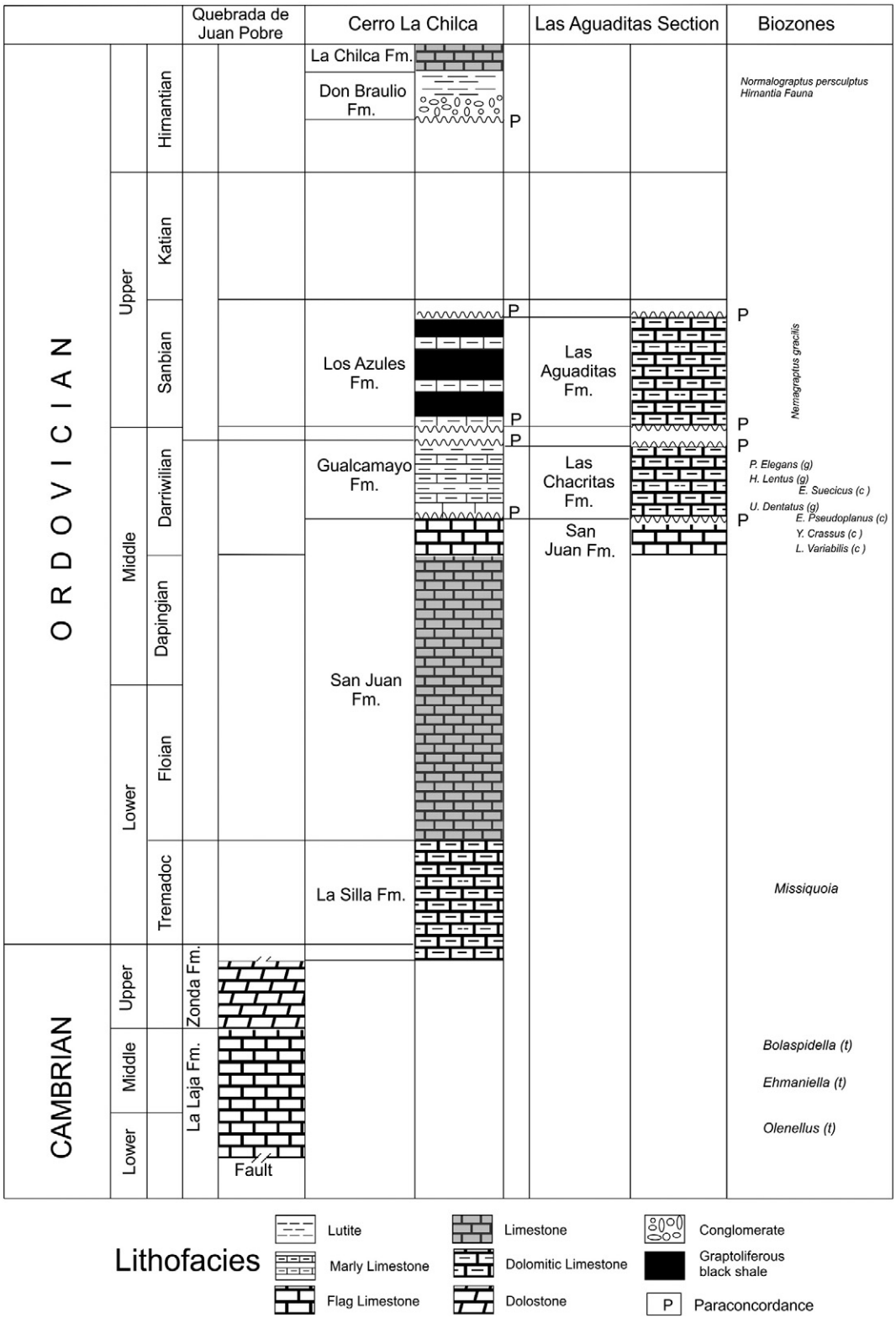

Fig. 3. Stratigraphic chart including Upper Cambrian and Ordovician formations from the three studied sections, including the recognized biozones (g = graptolite, c = conodont and t = trilobite).

fillings. This formation differs from the underlying La Silla Formation by the occurrence of an abundant and diverse open-sea fauna including trilobites, brachiopods, crinoids and sponges, among others (Peralta, 2003). Of particular interest for paleo-environmental reconstruction are reefal structures such as reef mounds composed of stromatoporoids, sponges, algae and receptaculitids (Cañas and Keller, 1993; Keller and Bordonaro, 1993). Microfossils are represented by algae and conodonts (Hünicken, 1989; Sarmiento, 1990; Lehnert, 1993, 1995).

The limestones are typical shelf sediments in origin, deposited well below the storm-weather wave-base, near the boundary between oxic

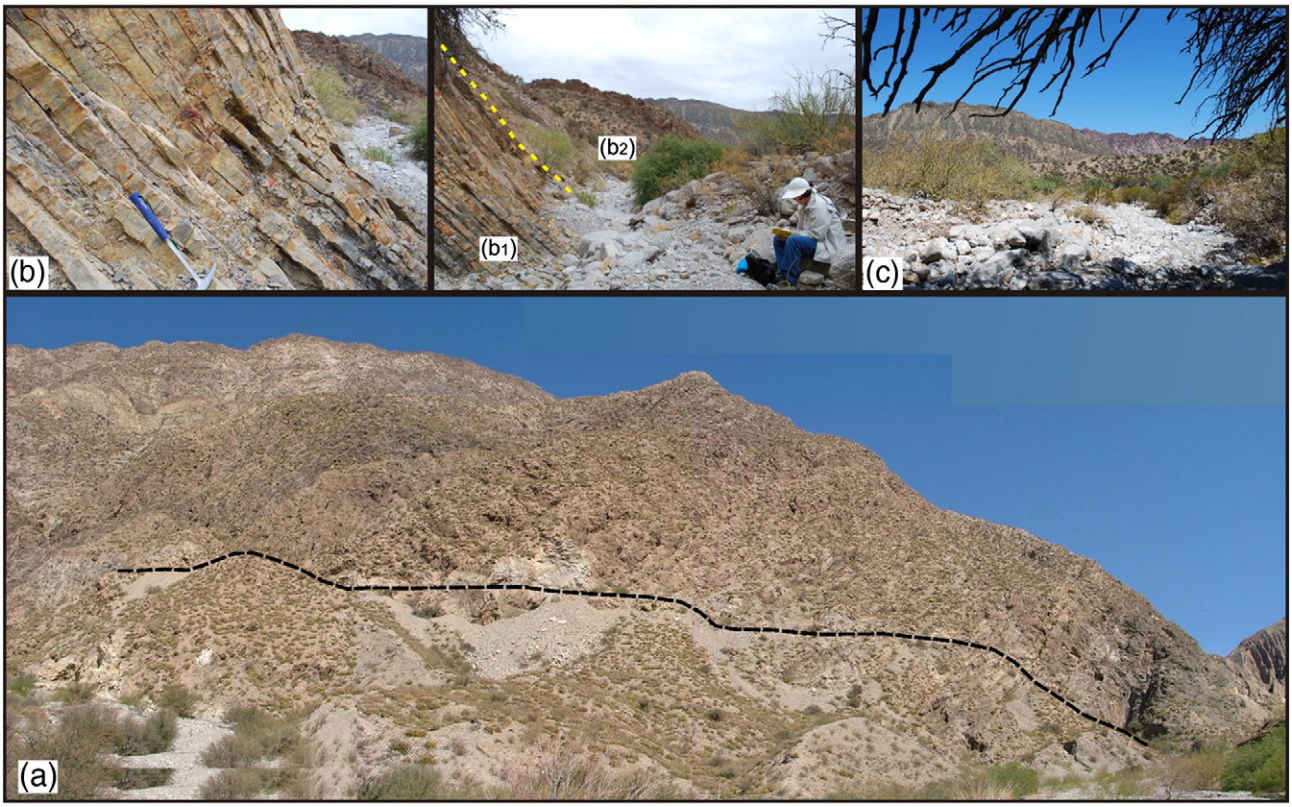

Fig. 4. Plate showing some of the major field aspects of the studied sections: (a) Quebrada de Juan Pobre where dashed line indicates the location of the section made; (b) Gualcamayo Formation; contact between the Gualcamayo (b_1) and Los Azules formations (b_2) and (c) Los Espejos Formation in the background.

and anoxic bottom conditions (Cañas, 1995) evidenced by rapid change from trilobite-rich layers to anoxic mudstones without ichnofossils record.

The Gualcamayo Formation, about 5 m thick, overlies paraconformably the San Juan Formation limestones. The lower member of the Gualcamayo Formation is composed of an alternation of black, tabular, marly limestones and dark, laminated shales with abundant shelly fauna, conodonts and graptolites. The top of this formation is characterized by a fossiliferous black limestone (Figs. 4 and 5) which is overlain by black shales of the Los Azules Formation. Whereas limestone beds of the Gualcamayo Formation contain conodonts, abundant trilobites and brachiopods, shales mostly bear graptolites. Cuerda (1986) based on graptolite biostratigraphy assigned it to the "early Llanvirn". A biostratigraphically well-constrained U–Pb zircon age of 464 ± 2 Ma for a K-bentonite layer (Huff et al., 1998) in the Gualcamayo Formation assigns this unit to the Darriwillian Stage.

Fig. 5. Rhythmites of the Gualcamayo Formation at the Cerro La Chilca section, Central Precordillera.

The Los Azules Formation is composed of about 80 m of graptolite-rich black shales with seven interbedded black limestone levels (Peralta, 1998, 2003; Fig. 4b). Limestone beds bear trilobites and conodonts that characterize the early "Caradoc" (= Sandbian Stage; *N. gracilis* biozone) age (Blasco and Ramos, 1976; Peralta, 1998). Cuerda and Furque (1985) observed an important hiatus between the top of the Gualcamayo Formation and the base of the Los Azules Formation. According to Peralta (2003), the whole euxinic sequence of the Los Azules Formation, very rich in organic remains, may be related to a global transgressive and anoxic event, and its facies sequence could be interpreted as a main rise of the sea level. A lowering of sea level happened in the Late Ordovician, during the Hirnantian glaciation (Peralta and Carter, 1990).

The Los Azules Formation (Fig. 4b_2) is disconformably (erosional surface) overlain by coarse debris-flow deposits of the late Hirnantian Don Braulio Formation (Astini and Benedetto, 1992; Peralta, 2003). Basal debris flows are mainly of calcareous clasts from underlying Ordovician units, but minor chert and siliciclast clasts are also observed.

The Cerro La Chilca section is the type locality of the Tucunuco Group (Cuerda, 1969), about 370 m thick, including the lower La Chilca (late Hirnantian–early Wenlockian) and upper Los Espejos (Mid Wenlockian–Ludlowian; Cuerda, 1969; Cuerda et al., 1982) or up to early Lochkowian (Benedetto et al., 1992) (Fig. 4c) formations (Cuerda, 1965, 1966, 1969).

2.4. Central Precordillera: Las Aguaditas Section (Ordovician)

A carbonate and mixed succession of Ordovician age is exposed along the Las Aguaditas section at the Los Blanquitos Ridge, Central

Table 1
C, O and Sr isotope analyses for carbonate samples from Quebrada de Juan Pobre (Cambrian), Cerro La Chilca and Río Las Aguaditas (Ordovician) sections.

Quebrada de Juan Pobre						Cerro La Chilca						Cerro Las Aguaditas					
Sample		Height * (m)	$\delta^{13}C$ ‰$_{VPDB}$	$\delta^{18}O$ ‰$_{VPDB}$	$^{87}Sr/^{86}Sr$	Sample		Height* (m)	$\delta^{13}C$ ‰$_{VPDB}$	$\delta^{18}O$ ‰$_{VPDB}$	$^{87}Sr/^{86}Sr$	Sample		Height (m) *	$\delta^{13}C$ ‰$_{VPDB}$	$\delta^{18}O$ ‰$_{VPDB}$	$^{87}Sr/^{86}Sr$ (1σ)
Laja	QJPZ-1	0	−0.5	−7.8		La Silla Formation	QLC1	0	−0.08	−6.11		Las Chacritas Formation	RLA1	0	−0.32	−5.50	
Zonda Formation	QJPZ-2	2	−0.4	−7.8			QLC2	5.5	0.18	−6.25			RLA2	2	−0.47	−6.33	
	QJPZ-3	5	−0.3	−7.7			QLC3	5	−0.08	−6.24			RLA3	20.5	−3.68	−6.53	
	QJPZ-4	3	0.3	−7.3			QLC4	5	−0.06	−6.06			RLA4	5	−1.43	−5.78	
	QJPZ-5	3	0.2	−7.4	0.7098		**QLC5**	8	−0.04	−6.30			RLA5	6	−0.35	−5.45	
	QJPZ-6	5	0.3	−7.9			QLC6	5	0.04	−6.06			RLA6	5	−0.54	−5.62	
	QJPZ-7	10	0.8	−6.4	0.7098		QLC7	5	−0.11	−6.36			RLA7	11	−0.76	−5.93	
	QJPZ-8	3	0.6	−7.9	0.7103		QLC8	5	−0.19	−6.48			RLA8	10.5	−1.35	−5.82	0.7092
	QJPZ-9	4.2	0.1	−7.3	0.7099		QLC9	5	−0.57	−6.32			RLA9	4.5	−1.80	−5.65	
	QJPZ-10	6.5	0.9	−6.3			QLC10	5	−0.07	−4.75			RLA10	4.5	−0.80	−5.36	
	QJPZ-13	5	0.6	−7.7		San Juan Formation	QLC11	5	0.59	−4.39			RLA11	3	−1.33	−5.20	
	QJPZ-14	5	0.2	−7.9			QLC12	5	−0.57	−6.02			RLA12	1.8	−1.02	−5.20	
	QJPZ-15	5	0.6	−7.5	0.7104		QLC13	7	−0.56	−6.14			RLA13	1	0.21	−5.11	
	QJPZ-16	5	0.2	−7.8			QLC14	5	−0.54	−6.28		Las Aguaditas Formation	RLA14	6	0.42	−4.95	
	QJPZ-17	2	0.4	−7.4			**QLC15**	5	−0.58	−6.16			RLA15	20	0.14	−5.00	
	QJPZ-18	3	0.6	−6.0			QLC16	5	−0.35	−5.95			RLA16	15.5	0.88	−5.02	
	QJPZ-19	2.8	0.4	−5.9			QLC17	5	−0.67	−6.03	0.7090		RLA17	27.5	0.90	−5.14	
	QJPZ-20	4.3	0.0	−5.8			QLC18	5	−0.65	−6.34			RLA 18	8	1.01	−5.12	
	QJPZ-21	4	−0.1	−5.4			QLC19	5	−0.71	−6.54			RLA19	5.5	1.06	−4.88	
	QJPZ-22	3	−0.6	−6.5			QLC20	5	−0.74	−6.40			RLA20	5	1.17	−5.31	
	QJPZ-23	4.5	−0.2	−5.9	0.7107		QLC21	5	−0.51	−6.31			RLA21	5	1.11	−5.45	
	QJPZ-24	4.6	−0.4	−4.7	0.7109		QLC22	5	−0.80	−6.25	0.7108		RLA22	5.5	0.81	−5.32	
	QJPZ-25	2.5	−0.4	−5.7			QLC23	5	−0.86	−6.24			RLA23	6	1.03	−5.41	
	QJPZ-26	10.3	−0.1	−5.3			QLC24	5	−0.84	−6.49			RLA24	6	1.95	−4.98	
	QJPZ-27	3	−0.7	−5.7			QLC25	5	−0.76	−6.15			RLA25	6	1.82	−5.43	
	QJPZ-28	5.5	−0.9	−4.9			QLC26	5	−0.74	−6.10	0.7089		RLA26	5	1.12	−5.46	
	QJPZ-29	5.5	−0.6	−5.7			QLC27	5	−0.95	−6.31			RLA27	5	1.24	−5.17	
	QJPZ-30	2.1	−0.8	−5.5			QLC28	5	−0.70	−6.38			RLA28	5	1.02	−3.76	
	QJPZ-31	3.5	−0.8	−5.9			QLC29	5	−0.82	−6.42			RLA29	9	0.53	−5.20	

QJPZ-32	9	−0.9	−6.0	0.7106		QLC30	5	−0.87	−6.01		RLA30	6	0.81	−5.49
QJPZ-33	3	−0.8	−4.9			QLC31	5	−0.95	−6.29		RLA31	5	1.33	−4.55
QJPZ-34	3	−0.7	−6.5			QLC32	5	−1.04	−6.51		RLA32	17	1.07	−4.88
QJPZ-35	3.5	−0.7	−5.5			QLC33	5	−1.12	−6.36		RLA33	6	0.87	−5.07
QJPZ-36	4.5	−0.6	−5.4	0.7109		QLC34	10	−1.43	−6.67		RLA34	20	0.63	−5.24
QJPZ-37	3	−1.0	−6.1	0.7104		QLC35	5	−1.46	−6.35		RLA35	5	0.50	−5.43
QJPZ-38	7.3	−1.0	−5.3	0.7104		QLC36	5	−1.46	−6.43		RLA36	6	1.27	−4.08
QJPZ-39	12	−1.0	−5.7			QLC37	5	−1.58	−7.85		RLA37	21	0.46	−5.42
QJPZ-40	3	−0.5	−5.2	0.7106		QLC38	10	−1.51	−6.32		RLA38	8.5	1.46	−4.09
QJPZ-41	4	−1.1	−5.2			QLC40	10	−1.51	−6.33		RLA39	7	0.27	−5.45
QJPZ-42	3	−1.9	−6.8			QLC41	10	−1.36	−6.51		RLA40	8.5	0.69	−5.52
QJPZ-43	4	−1.6	−6.4			QLC42	10	−1.26	−6.29		RLA41	6.5	0.71	−5.57
QJPZ-44	5	−1.2	−5.8			QLC43	10	−0.89	−6.35		RLA42	6	0.63	−6.41
QJPZ-45	4	−1.9	5.7			QLC44	1.5	−1.85	−5.96		RLA43	6	0.88	−5.28
QJPZ-46	10	−1.0	−5.3	0.7103	Los Azules Formation	QLC45	0.20	−1.64	−5.91		RLA44	20	1.13	−5.59
QJPZ-47	3	−1.0	−5.2			QLC46	4.3	−0.87	−5.46		RLA45	20	0.07	−6.24
QJPZ-48	4	−1.1	−7.7			QLC47	3	−2.57	−7.70		RLA46	21	0.26	−7.34
QJPZ-49	4	−0.9	−6.7			QLC48	2	−2.94	−5.48		RLA47	15	1.11	−5.47
QJPZ-50	5	−0.6	−7.1	0.7105		QLC49	3	−2.18	−5.98		RLA48	15	0.83	−5.45
QJPZ-51	4	−0.8	−6.9			QLC50	15	−2.18	−6.52					
QJPZ-52	3	−0.8	−6.9			QLC51	7.5	1.49	−2.23					
QJPZ-54	4	−0.7	−6.1			QLC52	9	1.57	−3.00					
QJPZ-55	4	−1.1	−6.2			QLC53A	30	2.80	−2.56					
QJPZ-56	3.5	−1.0	−6.1			QLC53B	1	−1.99	−6.73					
QJPZ-57	3.5	−0.7	−5.1			QLC54	23.5	1.35	−6.29					
QJPZ-58	3	−0.8	−6.0			QLC 54B	15	6.18	−2.10					
QJPZ-59	4	−1.1	−5.6			QLC55	13	0.45	−4.55					
QJPZ-60	3.5	−1.7	−8.1		La Chilca Formation	QLC56	10	−2.33	−0.23	0.7122				
QJPZ-61	4	−0.5	−5.7			QLC57	10	0.90	−5.11					
QJPZ-62	3	−0.5	−4.9	0.7106		QLC58	50	−2.99	−9.54					
QJPZ-63	3	−1.0	−5.8											
QJPZ-64	3	−1.1	−6.6	0.7108										

Table 2
Major (wt.%) and trace (ppm) chemical analyses, Quebrada de Juan Pobre, Precordillera.

Quebrada de Juan Pobre													
	QJPZ-1	QJPZ-4	QJPZ-5	QJPZ-7	QJPZ-8	QJPZ-9	QJPZ-10	QJPZ-15	QJPZ-18	QJPZ-22	QJPZ-23	QJPZ-24	QJPZ-25
SiO_2	3.85	1.12	0.98	1.26	0.97	1.26	1.45	1.3	1.5	2.46	1.51	3.10	1.71
Al_2O_3	1.29	0.41	0.29	0.44	0.26	0.35	0.47	0.34	0.33	0.57	1.10	0.72	0.72
Fe_2O_3T	0.62	0.2	0.31	0.23	0.24	0.27	0.22	0.19	0.22	0.38	2.10	2.00	0.51
MgO	1.51	1.34	1.42	4.14	3.36	3.57	9.08	10.99	9.45	20.06	22.40	22.52	20.86
CaO	50.38	54.07	54.77	51.07	53.58	52.99	45.89	44.29	45.56	31.28	26.79	25.44	34.51
Na_2O	–	–	0.17	–	0.22	0.15	0.03	0.19	0.2	–	0.31	0.32	0.27
K_2O	0.52	0.18	0.12	0.22	0.14	0.16	0.01	0.05	0.04	0.23	0.14	0.06	0.14
TiO_2	0.08	0.02	–	0.03	–	–	0.01	0.01	0.01	0.04	–	–	–
P_2O_5	0.03	0.02	0.01	0.01	0.01	0.01	–	–	–	–	0.07	0.08	0.01
CO_2	41.74	44.03	43.29	43.73	43.44	42.29	44.1	44.43	44.12	46.31	45.62	45.40	41.32
Total	100.04	101.4	101.37	101.13	102.23	101.04	101.25	101.79	101.43	101.34	100.58	100.17	100.06
Mn	163	67	60	60	60	60	43	31	42	44	385	380	60
Sr	689	706	584	606	302	436	402	295	354	159	119	93	164
Rb	5	5	3	5	1	3	5	4	6	5	4	1	5
Mg/Ca	0.02	0.02	0.02	0.06	0.04	0.05	0.16	0.20	0.17	0.55	0.71	0.75	0.51
Mn/Sr	0.23	0.09	0.10	0.09	0.19	0.14	0.10	0.11	0.12	0.27	3.23	4.08	0.36

Precordillera. Therein, the Early Ordovician San Juan Formation, the graptolite-rich Las Chacritas Formation (correlated to Gualcamayo Formation) and the Upper Ordovician Las Aguaditas Formation (Fig. 3) are well exposed in a continuous Ordovician succession. The Las Aguaditas Formation is correlated with the Los Azules Formation (Peralta, 1998). The difference between Cerro La Chilca and Los Blanquitos deposits is that the latter is shallower than equivalent formations at the Cerro La Chilca (Peralta and Rosales, 2007).

From a stratigraphic and sedimentologic point of view, these Upper Ordovician fine-grained deposits are similar to the Pelagic Carbonate Platform facies (PCP facies in the sense of Santantonio, 1994). Two successive pelagic facies are recognized: the first one is composed of carbonate and mixed fine-grained facies of the Las Aguaditas Formation in the Los Blanquitos–La Trampa block, which bears graptolites of the *N. gracilis* zone (Brussa, 1997), but similar deposits also occur in the younger, middle–upper Katian, Sassito Formation (Lehnert, 1995). The second facies is dominated by a thick package of Sandbian to Katian graptolite-rich black shale of the Los Azules Formation accumulated on the Cerro del Fuerte–Cerro La Chilca block.

The San Juan and Gualcamayo formations are mainly composed of limestones. Presence of bioclasts characterizes the base of Las Aguaditas Formation, showing conspicuous slump structures of a few meters which, sometimes, pose some difficulty in determining stratigraphic position of rocks being sampled. At the top, Las Aguaditas Formation is paraconformably (erosional surface) overlain by a basal cherty pebbly conglomerate of the late Hirnantian–early Wenlockian La Chilca Formation (Peralta, 2003).

3. Isotope geochemistry

3.1. Sampling and methods

It is known that at times of rapid environmental change, chemostratigraphy backed by biostratigraphy can enable correlation at much higher resolution than biostratigraphy alone (Brenchley et al., 2003). We have examined and collected samples along sections perpendicular to the strike of the carbonate strata, in meter intervals at Quebrada de Juan Pobre, at Cerro La Chilca and at Los Blanquitos Ridge. All these samples have been analyzed for carbon and oxygen isotopes while strontium isotope ratios have been determined in a total of 23 samples. Neodymium isotopes were analyzed only in 5 samples.

Analyses of C and O isotopes of carbonates were performed at the Stable Isotope Laboratory (LABISE) of the Department of Geology, Federal University of Pernambuco, Brazil. Extraction of CO_2 gas from micro-drilled powder (1 mm drill bit was used, avoiding fractures, recrystallized portions and weathered surfaces) was performed in a high vacuum line after reaction with 100% orthophosphoric acid at 25 °C for 1 day (3 days allowed, when dolomite was present). Released CO_2 was analyzed after cryogenic cleaning in a double inlet, triple-collector SIRA II or Delta V Advantage mass spectrometers and results are reported in δ notation in permil (‰) relative to the VPDB standard. The uncertainties of the isotope measurements were better than 0.1‰ for carbon and 0.2‰ for oxygen, based on multiple analyses of an internal laboratory standard (BSC).

For determination of the Sr isotopic ratios, powdered samples were leached in 0.5 M acetic acid and centrifuged to separate the soluble from the insoluble fractions. Strontium was eluted from solutions by ion-exchange chromatography using Sr-Spec resin. $^{87}Sr/^{86}Sr$ values were determined in static mode using a Finnigan MAT 262 seven-collector mass spectrometer at the University of Brasília, Brazil. The isotopic ratios were normalized to an $^{86}Sr/^{88}Sr$ value of 0.1194 and the 2σ uncertainty on Sr isotope measurements was less than 0.00009. Repeated analyses of NBS 987 standard indicated the value of 0.71024 ± 0.00007 (2σ) for the $^{87}Sr/^{86}Sr$ ratio.

For the same samples that were analyzed for Sr isotopes, major and some trace element concentrations were analyzed by X-ray fluorescence spectrometry, using fused beads and an automatic RIX-3000 (RIGAKU) unit available at the LABISE. Fused beads were prepared using Li fluoride and uncertainties were better than 5% for Sr and Fe and 10% for Mn. For all geochemical and isotope analyses in this study see Tables 1, 2, 3 and 4.

Nd isotopes were analyzed only in a few samples at the University of Copenhagen, Denmark. Two hundred milligrams of carbonate powder were added to an adequate amount of mixed $^{149}Sm–^{150}Nd$ spike and attacked by 2 mL of 0.5 mol L^{-1} acetic acid for 10 min. The supernatant was dried down and the solid was taken up in 300 μL of 2 mol L^{-1} HCl. Ion chromatographic separation took place first over a cation exchange column (separation of bulk REE), then over a column charged with Eichrom/Trischem's Ln-resin (to separate REE from each other) according to the procedure described by Kalsbeek and Frei (2010). Sm–Nd isotope measurements were made on an IsotopX/GV IsoProbe T thermal ionization mass spectrometer (TIMS). Sm–Nd isotope analyses were performed applying both static (Sm) and multidynamic (Nd) routines for the collection of the isotopic ratios. Nd isotope ratios were normalized to $^{146}Nd/^{144}Nd = 0.7219$. The mean value of $^{143}Nd/^{144}Nd$ for the JNdi-1 standard

QJPZ-26	QJPZ-28	QJPZ-32	QJPZ-33	QJPZ-36	QJPZ-37	QJPZ-38	QJPZ-40	QJPZ-42	QJPZ-46	QJPZ-50	QJPZ-57	QJPZ-62	QJPZ-64
4.27	1.07	1.02	0.96	3.66	3.81	1.01	1.73	1.88	0.17	0.04	0.79	0.77	0.63
0.46	0.44	2.22	0.75	0.23	0.67	0.46	0.73	0.92	0.08	0.01	0.39	0.12	0.02
0.39	0.29	0.33	0.58	0.3	1.22	0.29	0.46	0.4	0.17	0.13	0.35	0.26	0.19
20.77	21.34	22.67	22.95	21.03	23.14	22.45	19.11	20.24	20.32	21.28	20.8	21.54	23.22
30.35	33.43	35.27	34.04	31.68	36.46	35.98	34.04	33.16	34.69	33.27	35.1	35.77	36.76
–	–	0.20	0.19	–	0.40	0.23	–	–	–	–	–	0.23	0.27
0.2	0.13	0.12	0.23	0.11	0.07	0.11	0.22	0.29	–	–	0.09	0.02	0.03
0.04	0.04	0.01	–	0.02	–	–	0.06	3.05	0.01	0.01	0.03	–	–
0.01	0.01	–	0.02	–	0.09	0.01	–	0.01	–	0.01	–	0.01	0.01
45.02	41.07	40.10	41.28	44.71	35.56	40.85	45.23	41.65	46.14	46.78	44.15	42.81	40.05
101.52	101.79	101.95	101.01	101.75	101.88	101.39	101.59	101.6	101.58	101.53	101.7	101.52	101.18
59	51	60	55	52	350	50	46	37	25	27	36	55	60
117	311	233	167	205	99	360	337	364	315	272	358	313	302
5	4	4	6	5	3	4	5	5	5	–	5	3	3
0.57	0.51	0.54	0.57	0.55	0.54	0.53	0.47	0.50	0.49	0.50	0.47	0.60	0.53
0.50	0.16	0.25	0.33	0.25	3.53	0.13	0.14	0.10	0.08	0.09	0.10	0.18	0.20

(Tanaka et al., 2000) during the period of measurement was 0.512109 ± 0.000009 ($n = 5$).

3.2. Geochemical criteria of sample selection for C, O, Sr and Nd isotopes

Prior to the interpretation of the isotope data generated in this study, we review the more frequently used criteria for screening samples that have not undergone post-depositional alteration, as discussed below.

Concentration of Mn, Sr, Rb and Fe helps in selecting samples that have undergone little or no alteration (Kaufman and Knoll, 1995; Kah et al., 1999). The most effective parameter to screen primary values is the Mn/Sr ratio, because Sr is preferentially removed during recrystallization of meta-stable carbonate phases, while Mn becomes enriched during formation of late-stage ferroan calcite cement (Ripperdan et al., 1992; Derry et al., 1992; Kaufman et al., 1993; Knoll et al., 1995; Jacobsen and Kaufman, 1999).

Kaufman and Knoll (1995) stated that limestones or dolostones with Mn/Sr<10 commonly retain near primary $\delta^{13}C$ abundances. Limestones are considered to be unaltered only when Mn/Sr<1.5 and $\delta^{18}O > -10‰$ (VPDB) according to Fölling and Frimmel (2002). The Mn/Sr ratios for all but five samples in this study are <1.5 and $\delta^{18}O$ values for all samples are $> -10‰$ (VPDB).

In the cross-plot of $\delta^{18}O$ versus $\delta^{13}C$ in Fig. 6, the Quebrada de Juan Pobre and the Las Aguaditas sections show no clear co-variation between these two isotopes. However, the La Chilca section shows a co-variation pattern that could be explained as:

(a) Primary trend, where the heaviest $\delta^{18}O$ values occur just before and during the Hirnantian glaciation, as one would expect during glaciation. Light oxygen is trapped in the ice caps and the ocean shifts to more positive $\delta^{18}O$ values. If so, this shows that during cooling, a positive $\delta^{13}C$ excursion took place, i.e. the opposite of what happens in the Neoproterozoic;
(b) Consequence of compositional shift from limestone to dolostone;
(c) Result from both (preferable interpretation), the change in carbonate composition and the isotopes reflect paleoceanographic and climatic changes.

3.3. Quebrada de Juan Pobre Section: C and O isotopes

At Quebrada de Juan Pobre, sixty-four samples were collected in meter intervals (Fig. 2, Tables 1–2). This profile starts in the La Laja Formation (3 first samples) and all other samples are from the Zonda Formation. The last point sampled in this profile (sample QJP-64, Table 1) is located next to a fault that strongly affected the strata, the reason why the sampling was interrupted.

The obtained $\delta^{13}C$ stratigraphic profile shows a positive excursion (Fig. 7) in a fourfold-peak pattern. Upsection, the $\delta^{13}C$ stratigraphic pathway shows a negative excursion down to $-2‰$ (Fig. 7). Small negative shifts inside the positive excursion could be partially an artifact of diagenetic alteration. However, Mn/Sr ratios well below 1.0 seem to support near-primary signals.

The $\delta^{18}O$ curve in this section displays two plateaus, one around $-8‰$ at the basal portion of the Zonda Formation (coeval to the lower portion of a positive carbon isotope excursion), and another around $-5‰_{VPDB}$ towards the top, above this carbon isotope excursion. These $\delta^{18}O$ patterns are likely near-primary signals based on the following reasons: (a) $\delta^{18}O_{VPDB}$ values are all consistently $> -10‰$ in a range similar to that found for Upper Ordovician carbonates of Estonia and Latvia and regarded as near-primary values (e.g. Brenchley et al., 2003); (b) Mn/Sr ratios are less than 1.5 (except for one sample), and (c) the shape of the $\delta^{18}O$ and $\delta^{13}C$ stratigraphic curves are not sympathetic.

3.4. Cerro La Chilca and Las Aguaditas Sections: C and O isotopes

$\delta^{13}C$, $\delta^{18}O$, Ca/Mg and Mn/Sr for samples from the Cerro la Chilca are displayed in Fig. 8. The portion of the $\delta^{13}C$ stratigraphic profile corresponding to the La Silla Formation shows $\delta^{13}C$ values around 0‰ and at the transition to the San Juan Formation it exhibits a very discrete positive excursion (labeled I, Fig. 8). The samples from the San Juan Formation display a progressively more negative trend upsection up to the base of the Gualcamayo Formation, where a discrete positive excursion occurs (labeled II, Fig. 8). Positive shifts of $\delta^{13}C$ (Fig. 8) are observed upsection in the Los Azules Formation, with a peak around $+3‰$ (labeled III) followed by another peak of $+6‰$ (labeled IV).

The $\delta^{13}C$ curve for the Las Aguaditas section in the Los Blanquitos Ridge (Fig. 9) in which forty eight samples have been analyzed, reveals less vigorous fluctuations and four small positive isotope shifts (labeled I through IV). The base of this section (Las Chacritas Formation) yielded negative $\delta^{13}C$ values, but that together define a well-marked positive shift in this chemostratigraphic profile (labeled I, Fig. 9). A similar pattern is depicted in the $\delta^{13}C$ chemostratigraphic profile in the Gualcamayo Formation, labeled II, in Fig. 8 in the La Chilca Section,

Table 3
Major (wt.%) and trace (ppm) chemical analyses, Cerro La Chilca and Las Aguaditas sections, Precordillera.

Cerro La Chilca																			
	QLC 1	QLC 2	QLC 4	QLC 5	QLC 8	QLC 9	QLC 10	QLC 11	QLC 14	QLC 15	QLC 16	QLC 17	QLC 18	QLC 19	QLC 20	QLC 22	QLC 23	QLC 25	QLC 26
(a) Major elements																			
SiO_2	7.18	3.27	4.43	3.05	6.02	8.04	4.78	3.32	2.37	2.71	4.03	4.97	3.77	13.20	12.30	4.14	6.67	0.00	8.20
Al_2O_3	2.10	0.81	0.82	0.66	1.33	41.83	0.76	0.87	0.33	0.31	0.46	0.91	0.46	1.10	0.94	0.39	0.57	0.00	0.80
Fe_2O_3t	0.48	0.24	0.34	0.24	0.41	0.61	0.50	0.22	0.19	0.16	0.19	0.23	0.18	0.40	0.42	0.24	0.21	0.17	0.29
MgO	0.46	0.18	0.73	0.09	0.41	1.29	0.34	0.21	0.07	0.22	0.07	0.75	0.07	0.35	0.29	0.22	0.18	9.73	1.22
CaO	49.67	53.83	51.92	54.39	51.13	44.79	52.56	53.51	54.48	54.64	53.77	52.07	53.98	47.06	47.98	53.27	52.17	10.66	50.08
Na_2O	0.00	0.00	0.00	0.00	0.00	0.00	0.00	0.00	0.00	0.00	0.00	0.00	0.00	0.00	0.08	0.00	0.00	2.61	0.00
K_2O	0.38	0.07	0.05	0.01	0.12	0.24	0.01	0.04	0.00	0.00	0.00	0.04	0.00	0.07	0.05	0.00	0.00	2.91	0.02
TiO_2	0.07	0.03	0.03	0.02	0.04	0.07	0.03	0.03	0.01	0.01	0.01	0.03	0.01	0.04	0.04	0.01	0.02	3.19	0.03
P_2O_5	0.00	0.00	0.01	0.00	0.00	0.00	0.00	0.00	0.00	0.00	0.00	0.00	0.00	0.00	0.02	0.00	0.00	0.27	0.00
Mg/Ca	0.01	0.00	0.01	0.00	0.01	0.02	0.01	0.00	0.00	0.00	0.00	0.01	0.00	0.01	0.01	0.00	0.00	0.77	0.02
(b) Trace elements																			
Mn	317	232	255	263	224	216	294	170	185	162	193	201	193	131	147	201	178	77	239
Sr	336	316	315	329	321	260	326	377	406	373	322	347	368	2170	2108	413	375	1963	396
Rb	12	4	15	3	7	9	3	4	2	2	2	4	3	7	5	2	2	49	4
Mn/Sr	0.94	0.73	0.81	0.79	0.69	0.83	0.90	0.45	0.45	0.43	0.60	0.57	0.52	0.06	0.06	0.48	0.47	0.03	0.60

Table 3 (*continued*)

Cerro La Chilca																				
	QLC 27	QLC 28	QLC 30	QLC 38	QLC-40	QLC41	QLC-44	QLC-46	QLC-48	QLC-49	QLC 50	QLC 51	QLC 52	QLC 53	QLC 53B	QLC 54B	QLC 54	QLC 55	QLC 56	QLC 57
(a) Major elements																				
SiO_2	5.38	2.45	22.59	95.34	4.68	4.2	0	0	0	15.2	0	11.18	13.82	15.04	7.86	8.7	8.91	8.46	22.84	68.55
Al_2O_3	0.50	0.17	4.69	35.76	0.74	0.36	0	0	0	3.49	0	3.13	3.23	4.32	1.8	1.93	1.81	7.78	2.64	4.96
Fe_2O_3t	0.17	0.15	0.08	0.21	0.25	0.23	0.4	0.45	3.04	2.92	1.98	5.58	5.96	6.3	4.61	3.73	2.38	5.38	52.33	4.27
MgO	0.06	0.00	11.69	9.59	0.62	0.55	7.59	7.25	0	1.74	0	13.32	12.58	12.02	5.63	13.02	1.73	9.59	2.52	1.76
CaO	53.60	55.04	11.55	10.95	52.49	53.84	9.66	9.84	5.16	38.57	8.07	25.95	24.92	23.91	38.66	26.25	44.5	32.89	5.81	8.86
Na_2O	0.00	0.00	3.07	2.72	0	0	6.93	9.44	28.57	0.4	26.02	0.07	0.12	0.27	0.07	0.02	0.12	0.01	0	1.13
K_2O	0.00	0.00	0.29	2.90	0	0	18.24	20.03	53.59	0.52	39.97	0.63	0.63	0.86	0.28	0.33	0.22	0.02	0.33	0.45
TiO_2	0.02	0.01	1.08	2.05	0.03	0.02	7.19	7.47	0.22	0.24	4.1	0.28	0.28	0.36	0.15	0.23	0.15	0.06	0.38	0.58
P_2O_5	0.00	0.00	0.11	0.19	0	0	1.34	1.73	1.8	0.19	3.32	0.12	0.12	0.13	0.15	0.14	0.15	0.09	0.18	0.23
Mg/Ca	0.00	0.00	0.86	0.74	0.01	0.01	0.66	0.62	0.00	0.04	0.00	0.43	0.43	0.42	0.12	0.42	0.03	0.25	0.37	0.17
(b) Trace elements																				
Mn	178	154	77	77	154	154	232	232	464	1238	464	2244	1780	2012	1857	1161	1238	1393	1702	464
Sr	403	426	1784	1976	389	388	2234	3641	1994	737	2215	1392	1394	1460	1318	1621	921	1062	173	505
Rb	3	1	69	69	4	3	170	189	199	19	29	24	25	31	11	17	9	2	9	25
Mn/Sr	0.44	0.36	0.04	0.04	0.40	0.40	0.10	0.06	1.23	1.68	0.20	1.61	1.27	1.37	1.41	0.72	1.34	1.31	9.84	0.91

Table 3 (*continued*)

Las Aguaditas																				
	RLA 1	RLA 2	RLA 3	RLA 4	RLA 5	RLA 6	RLA 7	RLA 8	RLA 9	RLA 10	RLA 11	RLA 12	RLA 13	RLA 14	RLA 15	RLA 16	RLA 17	RLA 18	RLA 21	RLA 22
(a) Major elements																				
SiO_2	14.48	7.14	13.46	40.65	14.84	23.09	22.58	75.79	17.46	21.64	20.51	15.99	0.52	19.51	14.68	20.44	14.76	16.28	14.05	15.89
Al_2O_3	2.10	1.14	1.41	5.03	2.81	3.56	0.88	1.40	0.92	1.08	1.63	1.43	0.10	1.12	0.79	0.73	0.46	0.81	0.92	1.03
Fe_2O_3t	0.63	0.72	0.56	1.83	0.84	1.22	1.01	1.50	0.46	0.40	0.68	0.53	0.30	0.70	0.52	0.52	0.38	0.46	0.34	0.41
MgO	0.80	0.53	0.68	1.75	0.97	1.25	1.10	1.84	1.08	1.01	1.13	1.03	0.59	1.00	0.97	1.24	0.83	1.10	0.37	0.33
CaO	53.91	50.32	46.45	24.91	43.55	36.73	40.46	10.25	44.28	41.58	40.44	44.27	57.08	42.25	46.31	42.18	46.92	45.18	47.20	45.51
Na_2O	0.19	0.00	0.04	0.16	0.30	0.19	0.00	0.00	0.00	0.18	0.02	0.00	0.00	0.00	0.00	0.00	0.00	0.00	0.00	0.00
K2O	0.51	0.06	0.21	0.94	0.43	0.70	0.06	0.16	0.09	0.00	0.23	0.23	0.00	0.18	0.94	0.08	0.00	0.07	0.03	0.06
TiO_2	0.05	0.06	0.08	0.27	0.09	0.18	0.04	0.07	0.05	0.33	0.10	0.08	0.01	0.06	0.04	0.05	0.02	0.05	0.03	0.04
P_2O_5	0.58	0.34	0.03	0.04	0.01	0.02	0.01	0.00	0.00	0.00	0.01	0.01	0.05	0.00	0.00	0.00	0.00	0.01	0.00	0.01
Mg/Ca	0.01	0.01	0.01	0.06	0.02	0.03	0.02	0.15	0.02	0.02	0.02	0.02	0.01	0.02	0.02	0.02	0.01	0.02	0.01	0.01
(b) Trace elements																				
Mn	789	1602	766	379	301	340	232	178	270	232	394	309	294	789,48	160	766	116	131	139	131
Sr	538	526	640	684	848	830	1024	484	979	1418	944	623	542	1239	1174	1814	2108	1943	2202	2200
Rb	18	4	11	47	18	28	7	17	8	2	11	11	1	12	9	9	3	8	5	7
Mn/Sr	1.47	3.04	1.19	0.55	0.36	0.41	0.23	0.37	0.28	0.16	0.42	0.49	0.54	0.14	0.12	0.08	0.05	0.07	0.06	0.06

Table 3 (*continued*)

Las Aguaditas																				
	RLA 24	RLA 25	RLA 26	RLA 27	RLA 31	RLA 32	RLA 34	RLA 35	RLA 36	RLA 38	RLA 39	RLA 40	RLA 41	RLA 42	RLA 43	RLA 44	RLA 45	RLA 46	RLA 47	RLA 48
(a) Major elements																				
SiO_2	12.62	11.84	21.22	14.66	12.57	10.80	16.77	24.69	18.13	12.61	4.78	14.89	12.89	9.12	2.87	14.65	42.89	12.53	11.69	14.22
Al_2O_3	0.30	0.77	1.42	1.05	0.96	0.96	0.53	3.53	2.44	0.88	0.23	0.50	0.61	0.79	0.22	0.82	10.05	1.06	0.90	0.88
Fe_2O_3t	0.30	0.39	0.43	0.76	2.91	2.31	1.78	1.84	4.40	3.16	0.64	0.43	0.48	0.45	1.43	0.72	3.96	1.28	0.74	0.65
MgO	0.39	0.35	0.49	1.16	4.23	4.24	2.37	1.43	6.13	5.36	1.07	1.39	1.54	1.40	1.84	1.15	2.67	1.05	1.06	1.28
CaO	47.71	47.98	42.62	45.40	41.85	43.15	42.41	35.75	34.36	40.61	53.25	46.18	46.50	49.22	52.24	45.22	16.96	47.02	47.40	45.24
Na_2O	0.00	0.00	0.00	0.00	0.00	0.00	0.00	0.07	0.00	0.00	0.00	0.00	0.00	0.00	0.00	0.00	0.43	0.00	0.00	0.00
K2O	0.00	0.00	0.09	0.04	0.12	0.13	0.04	0.63	0.47	0.12	0.00	0.03	0.06	0.11	0.00	0.09	1.71	0.14	0.09	0.11
TiO_2	0.01	0.03	0.05	0.04	0.05	0.06	0.04	0.22	0.17	0.07	0.02	0.03	0.03	0.04	0.02	0.05	0.63	0.06	0.06	0.06
P_2O_5	0.02	0.03	0.02	0.03	0.06	0.06	0.08	0.04	0.10	0.15	0.03	0.00	0.00	0.00	0.02	0.03	0.10	0.08	0.04	0.01
Mg/Ca	0.01	0.01	0.01	0.02	0.09	0.08	0.05	0.03	0.15	0.11	0.02	0.03	0.03	0.02	0.03	0.02	0.13	0.02	0.02	0.02
(b) Trace elements																				
Mn	123	139	147	201	510	371	402	340	572	518	154	1315	132	132	209	170	309	217	170	163
Sr	2959	2506	2116	2415	2132	2236	2099	1530	1621	1896	1350	1793	1913	1492	1963	2036	900	2010	2227	2169
Rb	2	5	8	6	8	10	5	27	20	7	1	7	6	8	3	7	77	9	6	7
Mn/Sr	0.04	0.06	0.07	0.08	0.24	0.17	0.19	0.22	0.35	0.27	0.11	0.73	0.06	0.08	0.11	0.08	0.34	0.11	0.08	0.07

regarded as coeval to Las Chacritas Formation. Therefore, this positive excursion is unlikely to represent an artifact.

The $\delta^{18}O$ stratigraphic pathway in Fig. 8 displays one plateau around −6‰, corresponding to the San Juan and La Silla formations, and another portion of this pathway with vigorous fluctuations, $\delta^{18}O$ shifting to higher values in the Los Azules Formation. This abrupt change in the behavior of $\delta^{18}O$ is sympathetic with the onset of the carbon isotope excursions labeled II, II and IV.

The $\delta^{18}O$ stratigraphic pathway in Fig. 9, with all values > −10‰ VPDB, does not show much fluctuation except towards the top of the Las Aguaditas Formation. As the Mn/Sr ratios show values<1.0, except for three of them at the base of the section, we assume that the oxygen isotope ratios reported here are rather near-primary values. Sympathetic behavior of the $\delta^{18}O$ and the $\delta^{13}C$ stratigraphic pathways indicate slightly cooler temperatures during the time interval for the positive excursion labeled II, III and IV.

3.5. Sr and Nd isotopes

Strontium isotope ratios from seventeen samples from the Zonda Formation collected at the Quebrada de Juan Pobre section were analyzed (Table 1) and yielded $^{87}Sr/^{86}Sr$ values within a narrow range, from 0.7098 to 0.7109. Three samples of limestones of the La Laja Formation, from the base of the section, yielded values of 0.7098 (Table 2, Fig. 7) while dolostones of the Zonda Formation consistently displayed values above 0.7100 (0.7103 to 0.7109).

The $^{87}Sr/^{86}Sr$ ratios are slightly lower at the base of the profile (Juan Pobre Member) where limestones predominate and a bit higher upsection in the Zonda Formation, where dolostones predominate. Three values of $^{87}Sr/^{86}Sr$ for limestones of the Juan Pobre Member show very little variation (0.7098, 0.7098, 0.7099). Thirteen Sr isotope analyses for dolostones of the Zonda Formation display values from 0.7103 to 0.7109, all values too radiogenic to represent primary seawater composition. Although rocks sampled are essentially dolostones, twelve Sr isotope analyses exhibit a very narrow variation, suggesting that these rocks have faced only limited post-depositional alteration (Table 1).

A total of five samples from the Cerro La Chilca and Las Aguaditas sections were analyzed. At the Cerro La Chilca section, one sample from the La Silla Formation yielded a value of 0.7090 (Table 1), while one sample from the base of the San Juan Formation displayed a value of 0.7108 and another, collected 25 m upsection, yielded a value of 0.7089. A very high $^{87}Sr/^{86}Sr$ ratio was found for one sample from the top of the La Chilca Formation (0.7122).

These samples present Mn/Sr<1.5 and $\delta^{18}O$ > −10‰ VPDB, and this suggests they have escaped post-depositional alteration and, therefore, lowest $^{87}Sr/^{86}Sr$ ratios reported here are probably near-primary values and match the global curve in the Tremadocian–Darriwilian (McArthur et al., 2001).

A $^{87}Sr/^{86}Sr$ ratio of 0.7092 was determined for one sample from the Las Chacritas Formation at the Las Aguaditas section, a value that matches ratios of 0.7092 found at the top of San Juan Formation at Cerro La Chilca, near the contact with the Gualcamayo Formation (Table 1).

These Sr-isotope data, although limited, shows that the Argentine Precordillera recorded an important decrease of the seawater $^{87}Sr/^{86}Sr$ from the Upper Cambrian to the Middle Ordovician, in accordance with the global picture shown in Burke et al. (1982). Such a behavior probably reflects the influence of widespread volcanic activity from arc terranes present in low-latitude settings along eastern margins of Laurentia (e.g. Kolata et al., 1996), as well as explosive volcanism in Middle Ordovician in the Argentine Precordillera (e.g. Huff et al., 1998).

Five Sm–Nd isotope analyses were performed (Table 4) on samples that had been analyzed for Sr isotopes at the University of Copenhagen, Denmark. εNd (T) values were computed using the respective biostratigraphic ages.

Samples from the San Juan Formation (QLC-17, 22 and 26) yielded an εNd (T = 480 Ma) ranging between values of −10.06 and −4.83 and T_{DM} ages between 1.87 and 2.00 Ga. A sandstone with about 10% carbonate (QLC-56) from the top of Los Azules Formation, at the Cerro la Chilca section, yielded a εNd (T = 440 Ma) value of −5.24 and a T_{DM} age of 1.87 Ga. Finally, a sample from the Las Chacritas Formation (chronocorrelated to Gualcamayo Formation; RLA-8) from the Los Blanquitos Ridge yielded εNd (T = 470 Ma) of −7.55 and a T_{DM} age of 1.97 Ga.

Thus, a scattering in T_{DM} ages (1.87 to 2.00 Ga) and εNd values (−10.06 to −4.83) either reflect poorly-mixed chemical versus detrital signals, changes in source areas and/or tectonic setting. In a previous neodymium survey on Middle to Upper Ordovician siliciclastic rocks of the Argentine Precordillera, Gleason et al. (2006) reported εNd values between −8 (Middle Ordovician) and −4 (Late Ordovician) that basically do not differ much from values reported here for this time interval.

The Ordovician seawater shows large variations in Nd isotopic compositions, with εNd values ranging from −22 to −8, as reported by Stille et al. (1992) and shown in Fig. 9. For the time span 400 Ma and 550 Ma, two paleogeography-dependent evolutionary trends of εNd values have been observed by Keto and Jacobsen (1987). These authors inferred two ocean basins between North America and Baltica separated by an island and/or shoal circulation barrier, the smaller Iapetus Ocean having εNd values ranging from −5 to −9 and the larger, coeval Pacific-Panthalassa Ocean, with εNd values ranging from −10 to −20.

The εNd data (7 samples) for the Middle to Upper Ordovician of the Argentine Precordillera from Gleason et al. (2006) combined with values (5 samples) from the present study seem to fit better the neodymium-isotope trend for the Iapetus Ocean (Fig. 10).

4. Discussion and conclusions

Definitely the easiest way to identify $\delta^{13}C$ excursions of a particular section is by correlating the corresponding biostratigraphy of this section with that of contemporaneous sections in other parts of the world with already identified $\delta^{13}C$ excursions. To help reaching this goal in this study, Fig. 1 shows the Ordovician stratigraphic diagnostic graptolite and conodont biozones (after Albanesi and Ortega, 2002; Young et al., 2008), Upper Cambrian trilobite biozones (Elrick et al., 2011) and the duration of known Upper Cambrian and Ordovician $\delta^{13}C$ excursions (SPICE, SNICE, MDICE, GICE, HICE), based on Finney et al.(1999), Saltzman et al. (2003), Bergström et al. (2006, 2010) and Sial et al. (2008). The available graptolite-conodont or trilobite biostratigraphic biozones for the studied sections are shown in Figs. 7, 8 and 9.

The presence of trilobites of the *Bolaspidella* (Bordonaro, 1990) biozone at the base of Zonda Formation and *dunderbergia* biozone towards the top of this formation in the Quebrada de Juan Pobre has led Keller (1999) to assign the deposition of this formation to the Steptoean Stage. Therefore, we assume that the positive $\delta^{13}C$ excursion observed in this section (Fig. 7) corresponds to the SPICE, with maximum discrete $\delta^{13}C$ value of +1‰, in contrast with SPICE maximum peak value reported by Sial et al. (2008) at Quebrada de La Angostura where $\delta^{13}C$ peak value is of about +5‰. The presence of stromatolites in some dolomitic limestones to dolostones of the Zonda Formation that coincides with small negative shifts within the SPICE interval, shown in Fig. 7 suggests vigorous environmental fluctuations during intervals of shallow deposition in this section. Likely, there was oxidation of significant amounts of organic matter in these intervals, a way to lower $\delta^{13}C$ according to Saltzman et al. (1998).

The presence of trilobite of the *Plethopeltis* cf. *P. saratogensis* biozone upsection in the overlying La Flecha Formation reported somewhere in the Argentine Precordillera (Sunwaptan Stage; Vaccari, 1994) suggests that the negative $\delta^{13}C$ (~−2‰; Fig. 7), with shorter duration than SPICE, probably corresponds to the SNICE. Therefore, SPICE and SNICE excursions, previously reported from the Precordillera by Sial et al.

Table 4
Sm–Nd isotope data for carbonate samples from the La Chilca (QLC) and Las Aguaditas sections (RLA).

Formation	Sample	Sm (ppm)	Nd (ppm)	$^{147}Sm/^{144}Nd$	$^{143}Nd/^{144}Nd$	T_{DM} Goldst	T_{DM} de Paolo	T_{CHUR}	ε(0)	age Ma	ε (age)	Nd initial
San Juan	QLC17	3.10	12.79	0.14721	0.512281	1.98	2.00	1.10	−6.96	480	−6.95	0.512279
	QLC 22	0.07	0.36	0.11402	0.511863	1.96	1.98	1.43	−15.11	480	−10.06	0.511505
	QLC 26	0.63	2.81	0.13578	0.512199	1.85	1.87	1.10	−8.56	480	−4.83	0.511772
Los Azules	QLC 56	3.76	17.00	0.13373	0.512172	1.85	1.87	1.13	−9.09	440	−5.24	0.511751
Las Chacritas (Gualcamayo)	RLA 8	1.34	6.39	0.12658	0.512031	1.95	1.97	1.32	−11.84	470	−7.55	0.511633

(2008), are shown here to occur in one single section. This pair of excursions, typical of the Late Cambrian, indicates that the deposition of the Zonda Formation at Quebrada de Juan Pobre started around 500 Ma (age of onset of SPICE).

The occurrence of the SNICE at the Quebrada de Juan Pobre reinforces that this excursion observed for the first time in the La Flecha Formation at a different section (Quebrada de La Flecha: Sial et al., 2008) is not an artifact, and together with SPICE are important tools in refining the stratigraphy of the Upper Cambrian. Moreover, the record of the SPICE in the La Flecha Formation at Quebrada de La Angostura and in the Zonda Formation at Quebrada de Juan Pobre, confirms the diachronism of deposition of these two formations as visualized by Keller (1999).

The oxygen-isotope pattern for the Quebrada de Juan Pobre section reflects, perhaps, an abrupt change to cooler temperatures upward section and/or of sea-level up-and-downs but with progressive lowering during the onset of deposition of the Zonda Formation followed by progressive rise at this portion of the basin in the Eastern Precordillera. In other words, the oxygen-isotope chemostratigraphy of the Zonda Formation at Quebrada de Juan Pobre may reflect continuous cooling from the peak of SPICE towards SNICE.

Oxygen-isotope trends and seawater temperature changes across SPICE in North America, based on $\delta^{18}O$ of apatitic inarticulate brachiopod (Elrick et al., 2011) revealed a negative oxygen isotope excursion in the Steptoean followed by a progressive increase of $\delta^{18}O$ towards the Sunwaptan, something that resembles the temperature variation pattern observed in Quebrada de Juan Pobre, within the SPICE–SNICE duration interval.

The Mg/Ca ratio curve in Fig. 7 shows an abrupt increase at about one third of the way to the top of this section due to a markedly change in the dolomite/calcite ratio. The difference in the mineral–water fractionation factor for these two mineral phases could enhance the difference between the $\delta^{18}O$ patterns for the SPICE and SNICE intervals and leading to a false idea on the thermal contrast between them. However, a close examination of the $\delta^{18}O$ and Mg/Ca ratio stratigraphic curves show that changes in Mg/Ca ratios are far more pronounced than in the $\delta^{18}O$ values. Besides, these two curves seem to be decoupled from each other in several portions. Therefore, it is assumed here that changes in $\delta^{18}O$ value in the SPICE–SNICE peak interval are more a reflection of temperature change than Mg/Ca ratio variation.

Strontium-isotope ratios for the Zonda Formation at Quebrada de Juan Pobre in the present study are slightly higher than values for the Zonda Formation at Quebrada de La Flecha reported by Sial et al. (2008) and the SPICE and SNICE exhibit $\delta^{13}C$ peak values less pronounced than expected. This isotopic behavior at Quebrada de Juan Pobre results, perhaps, from a combination of several factors including more restricted and more saline environment, affected by sea-level fluctuations.

The presence of graptolites of the *perassiograptus tentaculatus* (Peralta, 2003) and conodont *E. suecicus* (Heredia and Mestre, 2011; Mestre and Heredia, 2012) biozones in the Gualcamayo Formation in the Cerro La Chilca section (Fig. 8) and of the *variabilis* and *E. suecicus biozones* (Heredia and Mestre, 2011) in the Las Chacritas Formation (Fig. 9) indicate a Darriwilian age deposition for these two formations. It is likely that the discrete positive $\delta^{13}C$ excursion seen in the Gualcamayo Formation (Fig. 8) and in the Las Chacritas (Fig. 9) Formation corresponds to the MDICE.

The absence of the graptolite the *Dicellograptus anceps* (Katian) or *Normalograptus extraordinarius* or *Normalograptus persculptus* (Hirnantian) biozones in the Los Azules Formation, Cerro La Chilca section, has led Peralta and Finney (2002) to discard a Katian or Hirnantian age for the deposition of this formation and propose a hiatus between the Los Azules and the late Hirnantian Don Braulio formations. The graptolite *Nemagraptus gracilis* (early Sandbian) and *Climacograptus bicornis* (late Sandbian; reported from this formation in some other section in the Argentine Precordillera) biozones instead

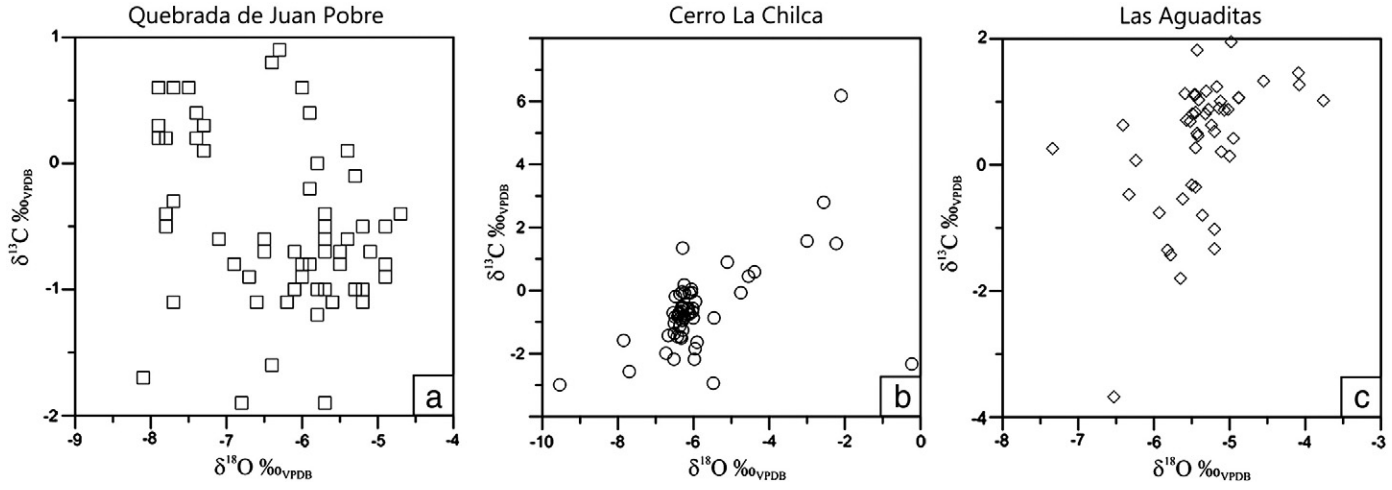

Fig. 6. Cross plot of $\delta^{18}O$ versus $\delta^{13}C$ for the three studied sections.

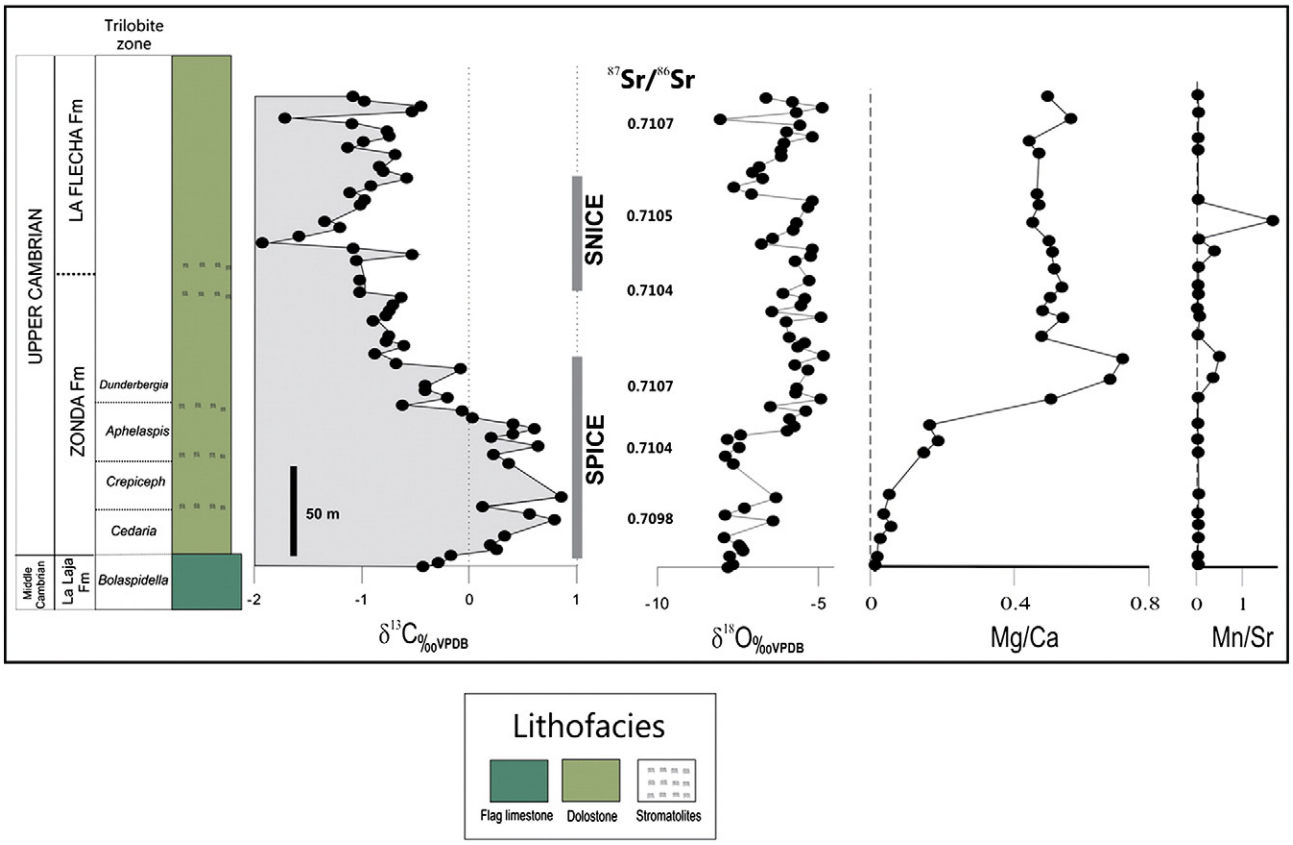

Fig. 7. C-, O- and Sr-isotope chemostratigraphic profile across dolostones of the Zonda Formation at Quebrada de Juan Pobre (Sierra Chica de Zonda), Eastern Precordilera. Trilobite zones are: *Biospidella* biozone (Baldis and Bordonaro, 1985; Bordonaro, 1990); *Cedaria*, *Crepiceph.*, *Aphelaspis*, *Dunderbergia* (Keller, 1999).

have been recognized (Peralta, 1995, 1998, 2003; Gleason et al., 2006) and a Sandbian age to this formation has been assigned.

The positive $\delta^{13}C$ excursion labeled IV in Fig. 8 in the upper portion of the Los Azules Formation within the *Climacograptus bicornis biozone* is interpreted here as the GICE and immediately precedes glacigenic rocks of the Don Braulio Formation, suggesting that enhanced organic carbon burial lowered atmospheric pCO_2 in preparation of the Hirnantian ice age. An impressive $\delta^{13}C$ negative excursion pre- and postdates the glacial horizon (Fig. 8), in a way that closely resembles Neoproterozoic glacial events (see for instance Halverson et al., 2010).

If the positive carbon isotope shifts labeled II, III and IV in the Las Aguaditas Formation in Fig. 9 are regarded together as the record of the GICE, this positive $\delta^{13}C$ excursion would be much larger (about 200 m) than described worldwide (including in the La Chilca section). Alternatively, we speculate if this set of positive shifts may correspond to a pre-GICE (II) positive excursion, within the *N. gracilis* biozone, and to the GICE (III + IV) excursion. The pre-GICE excursion could be an equivalent of the youngest (Spechts Ferry) of the four pre-GICE excursions, above the Deicke K-bentonite and below a negative shift beneath the point of the beginning of the GICE reported by Ludvigson et al. (2004) and Bergström et al. (2010) in North America. Up to now, kept as probably regional in nature, the Spechts Ferry excursion may prove to be of global occurrence.

This second hypothesis is preferable (abundant slumps in limestones of the Las Aguaditas Formation may be responsible for generating an apparent double peak, III and IV), and therefore the GICE is less pronounced in this profile than its record at the Cerro La Chilca, and with a more elevated baseline.

The difference of amplitude of the peak of the GICE excursion from the Cerro La Chilca to the Las Aguaditas sections is, perhaps, connected to differences in depth of sedimentation, allowing more oxidation of organic matter in the Las Aguaditas Formation, of shallower deposition, than in the Los Azules Formation of deeper sedimentation.

As the corresponding Mn/Sr ratios for the analyzed samples from the La Chilca and Las Aguaditas sections are <1.0, we assume that the oxygen isotope ratios reported in the present study for these two sections are near-primary ones. The $\delta^{18}O$ pathway for La Chilca section shows little Mg/Ca and $\delta^{18}O$ variations during the Early to Middle Ordovician but strong fluctuations of these two parameters, with much higher Mg/Ca ratios and higher $\delta^{18}O$ values, during the late Sandbian GICE and pre-GICE intervals.

In the Las Aguaditas section, there is much lower Ca/Mg variation and less pronounced $\delta^{18}O$ fluctuation to higher values in the late Sandbian Las Aguaditas Formation. In summary, the $\delta^{18}O$ patterns for the late Sandbian Los Azules and Las Aguaditas formations point to cooler temperatures during the GICE and pre-GICE intervals, but we cannot ignore some influence of the calcite/dolomite mineral–water fractionation factor, enhancing sometimes in the La Chilca section the difference in the $\delta^{18}O$ values.

As a major conclusion of this study, we can say that the carbon-isotope stratigraphy suggests that the Sandbian Stage in the Argentine Precordillera was characterized by highly fluctuating carbon-isotope values as observed in the Los Azules Formation, indicating climatic cyclicity and/or vigorous sea-level fluctuations, with important sea-level drop towards the end of the Hirnantian. No abrupt changes occur in the Dapingian portion of this carbon-isotope curve, but the mid-Darriwilian small positive excursion (likely MDICE) nearly coincides with a positive oxygen-isotope

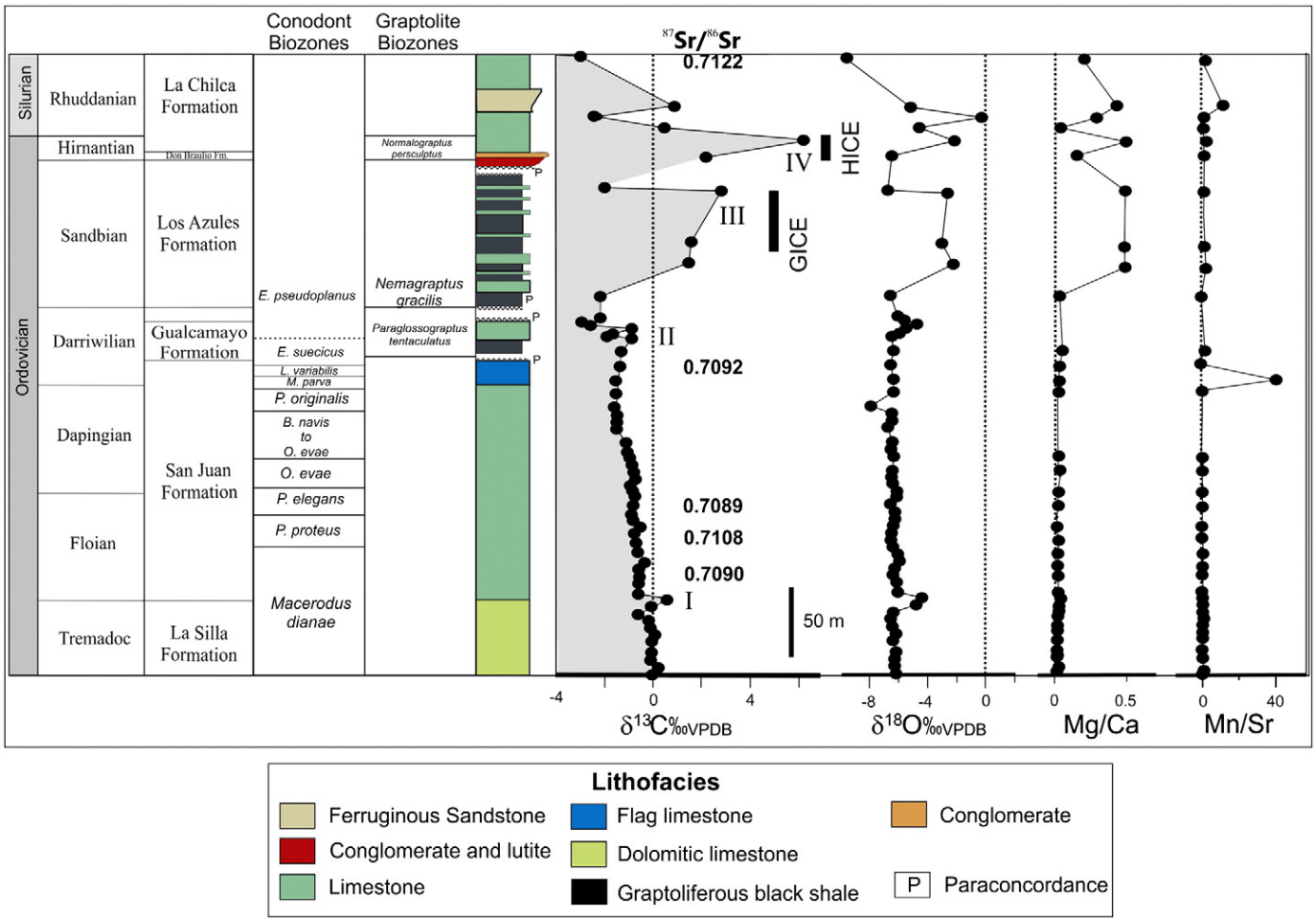

Fig. 8. Preliminary C-, O- and Sr-isotope composite variation curve for the Ordovician San Juan, Gualcamayo and Los Azules formations at the Cerro La Chilca, Central Precordillera. Conodont biozones were compiled from Buggisch et al. (2003) and Heredia and Mestre (2011). Graptolite biozones are from Peralta (1995, 1998, 2003) and Gleason et al. (2006). Hinantia fauna has been also recognized by Astini and Benedetto (1992).

excursion that, if near-primary, reflects onset of cooler sea-surface temperatures and biodiversification increase, pointing to a climatic background for this event.

Organic burial has led to large ^{12}C sequestration in the deep ocean during the Darriwilian and Sandbian stages in the Argentine Precordillera allowing for positive carbon isotope excursions (MDICE, pre-GICE and GICE). The deposition of the graptoliferous black shales of the Gualcamayo and Los Azules formations likely resulted from deep-ocean anoxia with saline bottom water as in the model proposed by Cramer and Saltzman (2005) to explain the early Wenlock positive carbon isotope excursion in North America.

In the Cerro La Chilca section, the fossiliferous Don Braulio Formation is late Hirnantian in age, and the basal conglomerate of the overlaying La Chilca Formation is latest Hirnantian in age according to the graptolite fossil record of *Normalograptus persculptus* biozone (Cuerda et al., 1988). The positive $\delta^{13}C$ excursion recorded in the basal portion of the La Chilca Formation followed by a negative shift reaching a value of −2‰, probably corresponds to the HICE (labeled IV, Fig. 8), in agreement with the current biostratigraphic knowledge.

The record of MDICE, GICE and HICE in South America reinforces their global nature. Together, these three positive carbon isotope excursions coupled with the occurrence of SPICE–SNICE in the Argentine Precordillera represent important chronostratigraphic tools that can help refine Upper Cambrian and Ordovician stratigraphies, as well as establishing regional and global, high-resolution correlations and sea-level change history.

5. Final remarks

The acronyms for the three Ordovician positive carbon-isotope anomalies deserve, perhaps, reconsideration. The denomination GICE has been given after the Gutenberg Member of the late Sandbian Decorah Formation, in which this anomaly was first documented. If one deals with an Ordovician formation, other than Sandbian in age, whose name starts with the letter "G" (e.g., Darriwillian Gualcamayo Formation), GICE could be a misleading denomination. Instead, SICE (Sandbian isotope carbon excursion), a denomination tied to the Stage in which it occurs, could avoid further confusion.

Likewise, it could be said in relation to the MDICE acronym, where "M" stands for Middle Ordovician that comprises two stages. DICE (Darriwilian isotope-carbon excursion) instead, could be perhaps more suitable.

Acknowledgments

We thank Gilsa Maria de Santana and Vilma Sobral Bezerra who have performed the C- and O-isotope analyses in this study, at the NEG-LABISE, Federal University of Pernambuco, Recife, Brazil. We also thank Natan Silva Pereira who performed the drafting of figures in

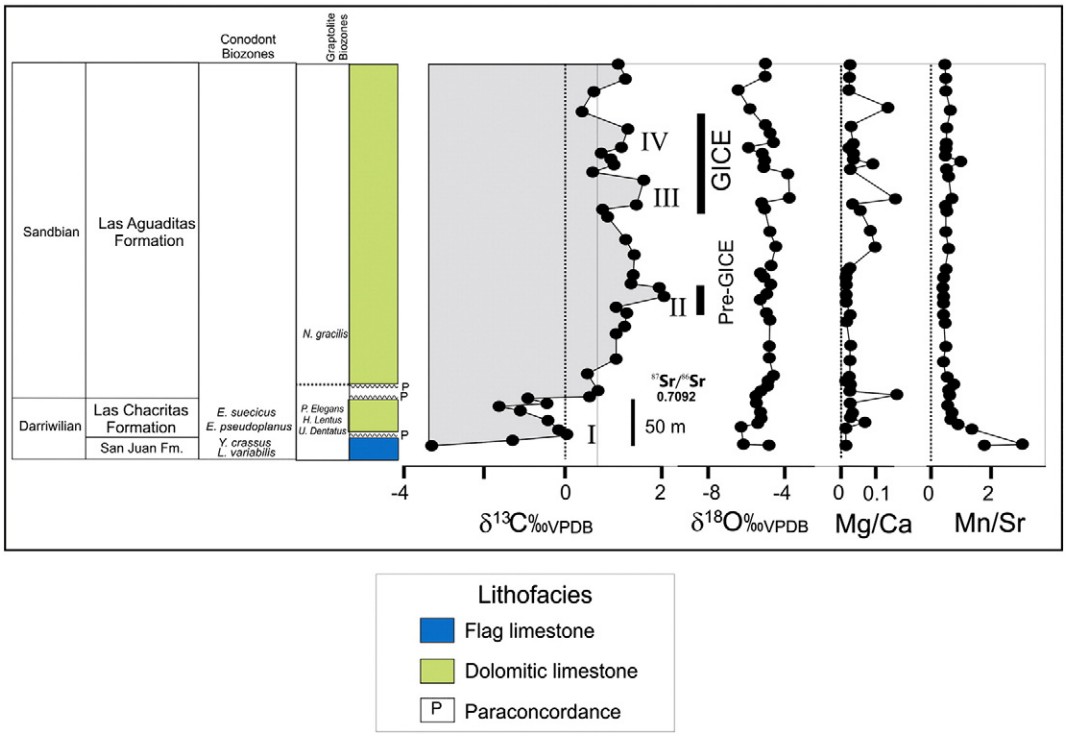

Fig. 9. C-, O- and Sr-isotope chemostratigraphic profile, at the Cerro Los Blanquitos (Río Las Aguaditas), near Jachal, Central Precordillera. Conodont biozones are from Heredia and Mestre (2011).

this paper. We are grateful to the Institute of Geology, National University of San Juan, Argentina, for sample preparation for geochemical and isotope analyses. We also thank the National Council for Scientific and Technological Development (PROSUL/CNPq 490136/2006 and CNPq 470399/2008) which financed the field work and FACEPE (APQ 0727-1.07/08), FACEPE-PRONEX (APQ-0479-1.07/06) which partially financed the laboratorial work. This is the scientific contribution no. 257 of the NEG-LABISE.

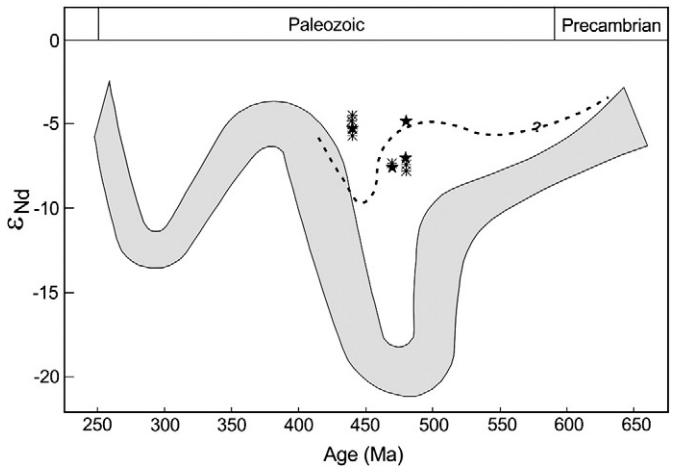

Fig. 10. εNd variation in the Paleozoic sea water (after Stille et al., 1992). εNd values are plotted vs. their stratigraphic age, the general trend (in gray) representing the Nd isotopic evolution in the Paicific–Panthalassa Ocean and the solid line, the Nd isotopic evolution in the Iapetus Ocean. Data from Gleason et al. (asterisk) and from this study (black stars) plot near the εNd variation trend for the Iapetus Ocean.

References

Aceñolaza, F.G., Toselli, A.J., 1999. Argentine Precordillera: allochthonous or autocthonous Gondwanic? Zentralblatt für Geologie und Paläontologie Teil II 7 (8), 1–14.
Ainsaar, L., Meidla, T., Martma, T., 1999. Evidence for a widespread carbon isotopic event associated with late Middle Ordovician sedimentological and faunal changes in Estonia. Geological Magazine 136, 49–62.
Ainsaar, L., Kaljo, D., Martma, T., Meidla, T., Männik, P., Nõlvak, J., Tinn, T., 2010. Middle and Upper Ordovician carbon isotope chemostratigraphy in Baltoscandia: a correlation standard and clues to environmental history. Palaeogeography, Palaeoclimatology, Palaeoecology 294, 189–201.
Albanesi, G.L., Ortega, G., 2002. Advances on conodont-graptolite biostratigraphy of the Ordovician System of Argentina. In: Aceñolaza, F.G. (Ed.), Aspects on the Ordovician System of Argentina: INSUGEO, Tucuman, Serie Correlación Geológica, 16, pp. 43–165.
Álvaro, J.J., Bauluz, B., Subias, I., Pierre, C., Vizcaino, D., 2008. Carbon chemostratigraphy of the Cambrian–Ordovincian transition in a midlatitude mixed platform, Montagne Noire, France. Bulletin of the Geological Society of America 120, 962–975.
Arroqui Langer, A., Bordonaro, O.L., 1996. Estratigrafía de la Formación Zonda (Cámbrico superior) en las sierras de Villicum y Zonda, Precordillera Oriental, Provincia de San Juan, Argentina. Actas VI Reunión Argentina de Sedimentología-I Simposio de Arcillas, Bahía Blanca, pp. 75–82.
Astini, R., Benedetto, J.L., 1992. El Ashgilliano tardío (Hirnantiano), del cerro La Chilca, Precordillera de San Juan, Argentina. Ameghiniana 29, 249–264.
Baldis, B.A., Bordonaro, O.L., 1985. A new interpretation of the fossiliferous Cambrian of Western Argentina. Cordoba, Boletín Academia Nacional de Ciencias, Tomo 56 (3–4), 297–307.
Baldis, B.A., Chebli, G., 1969. Estructura profunda del area central de la Precordillera sanjuanina. Actas 4tas. Jornadas Geológicas Argentina, I, Mendoza 47–66.
Baldis, B.A., Beresi, M.S., Bordonaro, O.L., Vaca, A., 1982. Síntesis evolutiva de La Precordillera Argentina. V Congreso Latinoamericano de Geología. Actas, Buenos Aires 4, 399–445.
Benedetto, J.L., Rachboeuf, P., Herrera, A., Brussa, E., Toro, B., 1992. Brachiopodes et bioestratigraphie de la Formacion de los Espejos, Siluro-Devonien de la Precordillere (NW Argentine). Geobios 25, 599–637.
Bergström, S.M., Saltzman, M.R., Schmitz, B., 2006. First record of the Hirnantian (Upper Ordovician) $\delta^{13}C$ excursion in the North American Midcontinent and its regional implications. Geological Magazine 143, 657–678.
Bergström, S.M., Schmitz, B., Saltzman, M.R., Huff, W.D., 2010. The Upper Ordovician Guttenberg $\delta^{13}C$ excursion (GICE) in North America and Baltosdcandia: occurrence, chronostratigraphic significance, and paleonevironmental relationships. The Geological Society of America, Special Paper 466, 37–67.
Blasco, G., Ramos, V., 1976. Graptolitos Caradocianos de la Formación Yerba Loca y del Cerro La Chilca, Departamento Jáchal, Provincia de San Juan. Ameghiniana 13, 312–329.

Bordonaro, O.L., 1990. Biogeografía de trilobites Cámbricos en La Precordillera Argentina. Universidad Nacional de Tucuman, Serie Correlación Geológica 7, 25–30.
Bordonaro, O.L., 2003a. Review of the Cambrian Stratigraphy of the Argentine Precordillera. Geológica Acta, Barcelona 1, 11–21.
Bordonaro, O.L., 2003b. Evolución Paleoambiental y Paleogeográfica de La Cuenca Cámbrica de la Precordillera Argentina. Revista de la Asociación Geológica Argentina, Buenos Aires 58, 329–346.
Brenchley, P.J., Garden, G.A., Hints, L., Kaljo, D., Marshall, J.D., Martma, T., Meidla, T., Nõlvak, J., 2003. High-resolution stable isotope stratigraphy of Upper Ordovician sequences: constraints in the timing of bioevents and environmental changes associated with mass extinction and glaciations. Geological Society of America Bulletin 111, 89–104.
Brussa, E.D., 1997. Las graptofaunas ordovícicas de la Formación Las Aguaditas, Precordillera de San Juan, Argentina. Parte II: Familias Cryptograptidae, Dicranograptidae, Diplograptidae y Orthograptidae. Ameghiniana 34, 93–105.
Buggisch, W., Keller, M., Lehnert, O., 2003. Carbon isotope record of Late Cambrian to Early Ordovician carbonates of the Argentine Precordillera. Paleogeography, Palaeoclimatology, Palaeoecology 195, 357–373.
Burke, W.H., Denison, R.E., Hetherington, E.A., Koepnick, R.B., Nelson, H.F., Otto, J.B., 1982. Variation of seawater $^{87}Sr/^{86}Sr$ throughout Phanerozoic time. Geology 10, 516–519.
Cañas, D., 1995. Early Ordovician carbonate platform facies of the Argentine Precordillera: restricted shelf to open platform evolution. In: Cooper, J.D., Droser, M.L., Fnney, S.C. (Eds.), Ordovician Odyssey: Short Papers for the Seventh International Symposium on the Ordovician System: Pacific Section SEPM (Society for Sedimentary Geology), Publication, 77, pp. 221–224.
Cañas, D., Keller, M., 1993. "Reefs" y "Reef Mounds" en la Formación San Juan (Precordillera Sanjuanina, Argentina): Los arrecifes más antiguos de Sudamérica. Boletín Real Sociedad Española de Historia Natural (Geologia) 88, 127–136.
Cramer, B.D., Saltzman, M.R., 2005. Sequestration of ^{12}C in the deep ocean during the early Wenlock (Silurian) positive carbon isotope excursion. Palaeogeography, Palaeoclimatology, Palaeoecology 219, 333–349.
Cuerda, A.J., 1965. Monograptus leintwardinensis var. incipiens Wood in El Silúrico dela Precordillera. Ameghiniana 4, 171–177.
Cuerda, A.J., 1966. Fomación la Chilca, Silurico Inferior-San Juan. Comisión de Investigaciones Científicas, La Plata, Notas IV (1), 1–12.
Cuerda, A., 1969. Sobre las graptofaunas del Silúrico de San Juan. Ameghiniana 6, 233–235.
Cuerda, A.J., 1986. Graptolitos del trecho de la Formación San Juan, Precordillera de San Juan. Actas Iv Congreso Argentino de Paleontologia y Bioestratigafia, Mendoza 1, 49–57.
Cuerda, A.J., Furque, G., 1985. Graptolitos del trecho de la Formación San Juan, Precordillera de San Juan. Actas Primeras, Jorn. Geol. Precordillera, Asoc. Geol. Argentina (ed) Serie A, Monografias y Reuniones 2, 113–118.
Cuerda, A.J., Furque, G., Uliarte, E., 1982. Graptolitos del base del Silurico de La Sierra deTalacasto, Precordillera de San Juan. Ameghiniana 19, 239–252.
Cuerda, A.J., Rickard, B., Cingolani, C.A., 1988. A new Ordovician–Silurian boundary section in San Juan Province, Argentine, and its definitive graptolite fauna. Journal of the Geological Society 145, 1–9.
Derry, L.A., Kaufman, A.J., Jacobsen, S.B., 1992. Sedimentary cycling and environmental change in the late Proterozoic: evidence from stable and radiogenic isotopes. Geochimica et Cosmochimica Acta 56, 1317–1329.
Droser, M.L., Bottjer, D.J., 1988. Trends in depth and extent of bioturbation in Cambrian carbonate marine environments, Western United States. Geology 16, 233–236.
Elrick, M., Rieboldt, S., Saltzman, M., McKay, M., 2011. Oxygen isotope trends and seawater temperature changes across the Late Cambrian Steptoean positive carbon-isotope excursion. Geology 39, 987–990.
Fan, J., Peng, P., Melchin, M.J., 2009. Carbon isotopes and event stratigraphy near the Ordovician–Silurian boundary, Yichang, South China. Palaeogeography, Palaeoclimatology, Palaeoecology 276, 160–169.
Finney, S.C., Berry, W.B.N., Cooper, J.D., Ripperdan, R.L., Sweet, W.C., Jacobson, S.R., Soufiane, A., Achab, A., Noble, P.J., 1999. Late Ordovician mass extinction: a new perspective from stratigraphic sections in central Nevada. Geology 27, 215–218.
Fölling, P.G., Frimmel, H.E., 2002. Chemostratigraphic correlation of carbonate succesions in the Gariep and Saldania Belts, Namibia and South Africa. Basin Research 13, 1–37.
Gill, B.C., Lyons, T.W., Saltzman, M.R., 2007. Parallel, high-resolution carbon and sulfur isotope records of the evolving Palaeozoic marine sulphur reservoir. Palaeogeography, Palaeoclimatology, Palaeoecology 256, 156–173.
Gleason, J.D., Finney, S.C., Peralta, S.H., Geherls, G.E., Marsaglia, K.M., 2006. Zircon and whole-rock Nd–Pb isotopic provenance of Middle and Upper Ordovician siliciclastic rocks, Argentine Precordillera. Sedimentology 1–30.
Halverson, G.P., Wade, B.P., Hurtgen, M.T., Barovich, K.M., 2010. Neoproterozoic chemostratigraphy. Precambrian Research 182, 337–350.
Haq, B.U., Schutter, S.R., 2008. A chronology of Paleozoic sea-level changes. Science 322, 64–68.
Hatch, J.R., Jacobson, S.R., Witzke, B.J., Risatti, J.B., Anders, D.E., Watney, W.L., Newell, K.D., Vuletich, A.K., 1987. Possible late Middle Ordovician carbon isotope excursion: evidence from Ordovician oils and hydrocarbon source rocks, Mid-continent and east-central United States. American Association of Petroleum Geologists Bulletin 71, 1342–1354.
Heredia, S., Mestre, A., 2011. Middle Darriwilian conodont biostratigraphy in Argentine Precordillera. Cuadernos del Museo Geominero 14, 237–242.
Huff, W.D., Davis, D., Bergström, S.M., Krekeler, M.P.S., Kolata, D.R., Cingolani, C.A., 1998. A biostratigraphically well-constrained K-bentonite U–Pb zircon age of the lowermost Darriwillian Stage (Middle Ordovician) from the Argentine Precordillera. Episodes 20, 29–33.
Hünicken, M., 1989. Some palegeographical aspects of South American conodonts and related forms. Courier Forschung Intitute Stenkeberg 117, 29–49.
Jacobsen, S.B., Kaufman, A.J., 1999. The Sr, C and O isotopic evolution of Neoproterozoic seawater. Chemical Geology 161, 37–57.
Jones, D.S., Fike, D.A., Finnegan, S., Fischer, W.W., Schrag, D.P., McCay, D., 2011. Terminal Ordovician carbon isotope stratigraphy and glacioeustatic sea-level change across Anticosti Island (Québec, Canada). Geological Society of America Bulletin 123, 1645–1664.
Kah, L.C., Sherman, A.G., Narbonne, G.M., Knoll, A.H., Kaufman, A.J., 1999. $\delta^{13}C$ stratigraphy of the Proterozoic Bylot Supergroup, Baffin Islands, Canada: implications for regional lithostratigraphy correlations. Canadian Journal of Earth Sciences 36, 313–332.
Kaljo, D., Hints, L., Martma, T., Nolvak, J., Oraspold, A., 2004. Late Ordovician carbon isotope trend in Estonia, its significance in stratigraphy and environmental analysis. Palaeogeography, Palaeoclimatology, Palaeoecology 210, 165–185.
Kaljo, D., Martma, T., Saadre, T., 2007. Post-Hunnebergian Ordovician carbon isotope trend in Baltoscandia, its environmental implications and some similarities with that of Nevada. Palaeogeography, Palaeoclimatology, Palaeoecology 245, 138–155.
Kalsbeek, F., Frei, R., 2010. Geochemistry of Precambrian sedimentary rocks used to solve stratigraphical problems: an example from the Neoproterozoic Volta basin, Ghana. Precambrian Research 176, 65–76.
Kaufman, A.J., Jacobsen, S.B., Knoll, A.H., 1993. The Vendian record of Sr and isotopic variations in seawater: implications for tectonics and paleoclimatic. Earth Planetary Sciences Letters 120, 409–430.
Kaufman, A.J., Knoll, A.H., 1995. Neoproterozoic variations in the C-isotopic composition of seawater: stratigraphic and biogeochemical implications. Precambrian Research 73, 27–49.
Keller, M., 1999. Argentine Precordillera. Geological Society of America Special Publication 341, (140 pp.).
Keller, M., Bordonaro, O., 1993. Arrecifes de estromatopóridos en el Ordovícico inferior del Oeste Argentino y SUS implicaciones paloegeográficas. Revista Española de Paleontologia 8, 165–169.
Keto, L.S., Jacobsen, S.B., 1987. Nd and Sr isotopic variations of early Paloezoic oceans. Earth Planetary Sciences Letters 84, 27–41.
Knoll, A.H., Kaufman, A.J., Semikhatov, M.A., 1995. The carbon isotopic composition of Proterozoic carbonates: Riphean successions from northwestern Siberia (Anabar Massif, Turukhansk Uplift). American Journal of Science 295, 823–850.
Knoll, A.H., Bambach, R.K., Canfield, D.E., Grotzinger, J.P., 1996. Comparative Earth history and Late Permian mass extinction. Science 273, 452–457.
Kolata, D.R., Huff, W.D., Bergstrom, S.M., 1996. Ordovician K-bentonites of Eastern North America. Geological Society of America Special Paper 313, 1–84.
Kump, L.R., Arthur, M.A., Patzkowsky, M.E., Gibbs, M.T., Pinkus, D.S., Shehan, P.M., 1999. A weathering hypothesis for glaciation at high atmospheric pCO_2 during the Late Ordovician. Palaeogeography, Palaeoclimatology, Palaeoecology 152, 173–187.
Lehnert, O., 1993. Bioestratigrafia de los conodontes arenigianos de La Formación San Juan en la localidad de Niquivil (Precordillera Sanjuanina, Argentina) y su correlación intercontinental. Revista Española de Paleontologia 10, 1–58.
Lehnert, O., 1995. Geodynamic processes in the Ordovician of the Argentine Precordillera: New biostratigraphic constraints. In: Cooper, J.D., Droser, M.L., Finney, S.C. (Eds.), Ordovician odyssey: Short papers for the Seventh International Symposium on the Ordovician System: Pacific Section: SEPM (Society for Sedimentary Geology), Publication, 77, pp. 75–80.
Ludvigson, G.A., Jacobsen, S.R., Witzke, B.J., González, L.A., 1996. Carbonate component chemostratigraphy and depositional history of the Ordovician Decorah Formation, Upper Mississipi Valley. Geological Society of America Special Paper 306, 67–86.
Ludvigson, G.A., Witzke, B.J., Schneider, C.L., Smith, E.A., Emerson, S.J., Gonzalez, L.A., 2000. A profile of the mid-Caradoc (Ordovician) carbon isotope excursion at the MacGregor Quarry, Clayton County, Iowa. Geological Society of Iowa Guidebook 70, 25–31.
Ludvigson, G.A., Witzke, B.J., Schneider, C.L., Smith, E.A., Emerson, S.J., Carpenter, S.J., Gonzalez, L.A., 2004. Late Ordovician (Turinian–Chatfieldian) carbon isotope excursions and their stratigraphic and paleoceanic significance. Palaeogeography, Palaeoclimatology, Palaeoecology 210, 187–214.
McArthur, J.M., Howarth, R.J., Bailey, T.R., 2001. Strontium isotope stratigraphy: LOWESS version 3: best fit to the marine Sr-isotope curve for 0–509 Ma and Accompanying look-up table for deriving numerical age. Journal of Geology 109, 155–170.
Melchin, M.J., Holmden, C.E., 2006. Carbon isotope chemostratigraphy in Arctic Canada: sea-level forcing of carbonate platform weathering and implications for Hirnantian global correlation. Palaeogeography, Palaeoclimatology, Palaeoecology 234, 186–200.
Melchin, M.J., Holmden, C., Williams, S.H., 2003. Correlation of graptolite biozones, chitinozoan biozones and carbon isotope curves through the Hirnantian. In: Albanesi, G.L., Beresi, S., Peralta, S.H. (Eds.), Ordovician from the Andes: Serie Correlación Geológica, 17, pp. 101–104.
Mestre, A., Heredia, S., 2012. Darriwilian species of Histiodella (Conodonta) in the Argentine Precordillera. Alcheringa: An Australasian Journal of Palaeontology 36, 141–150.
Montañez, I.P., Banner, J.L., Mack, L.E., Musgrove, M., Osleger, D.A., 2000. Evolution of the Sr and C isotope composition of Cambrian oceans. GSA Today 10, 1–7.
Munnecke, A., Calner, M., Harper, D.A.T., Servais, T., 2010. Ordovician and Silurian sea-water chemistry, sea level, and climate: a synopsis. Palaeogeography, Palaeoclimatology, Palaeoecology 296, 389.
Orth, C.J., Gilmore, J.S., Quintana, L.R., Sheehan, P.M., 1986. Terminal Ordovician extinction: Geochemical analysis of the Ordovician/Silurian boundary, Anticosti Island, Quebec. Geology 13, 433–436.
Ortiz, A., Zambrano, J.J., 1981. La Provincia Geológica Precordillera Oriental. VIII Congreso Geológico Argentino, San Luis 3, 59–74.
Peng, S., Babcock, L., 2008. Cambrian period. In: Ogg, J.G., Ogg, G., Gradstein, F.M. (Eds.), The Concise Geologic Time Scale. Cambridge University Press, Cambridge, pp. 37–46.

Peralta, S.H., 1995. La Formación Gualcamayo en la Sieera de Villicum: sus graptolitos y faunas asociadas. Boletín de La Academía Nacional de Ciencias de Cordoba 60, 401–408.
Peralta, S.H., 1998. Graptolites of the Nemagraptus gracilis Zone in the Black sale sequences of the San Juan Precordillera, Argentina: its biostratigraphic and paleoenvironmental significance. In: Gutierrez-Marco, J.C., Rábano, I. (Eds.), Proceedings of the Sixth International Graptolite of the GWC (IPA) and the 1998 Field Meeting International Subcommission the Silurian Stratigraphy (ICS-IUGS), Madrid: Temas Geológico-Minero, 23, pp. 244–247.
Peralta, S.H., 2003. The Cerro La Chilca, Central Precordillera, San Juan Province. Ordovician and Silurian of the Precordillera of Argentina, San Juan, Argentina. Tucuman, INSUGEO. Miscelánea 10, 45–63.
Peralta, S.H., Carter, C.H., 1990. La glaciación Gondwanica del Ordovícico tardio: Evidencias en fangolitas guijarrosas de la Precorillera de San Juan. XI Congreso Geológico Argentino, Actas 2, 181–185.
Peralta, S.H., Finney, S.C., 2002. The Upper Ordovician graptolite faunas of the Cuyania Terrane: their biostratigraphic and Paleogeographic significance in the Western margin of Gondwana. In: Aceñolaza, F.G. (Ed.), Aspects of the Ordovician System in Argentina: Serie Correlación Geológica INSUGEO, 16, pp. 41–70.
Peralta, S.H., Rosales, C.V., 2007. Extensional tectonic controlling the Ordovician evolution of Precordillera Terrane, Western Argentina. Proceedings, 10th International Symposium on Ordovician System, Nanking, China, June 27–30.
Ramos, A.M., Valencio, S.A., Panarello, H.O., Armella, C., Cabaleri, N., 1999. Isotope and trace elements evidences of post-depositional changes in carbonates of La Flecha Formation, San Juan, Argentina. II South American Symposium on Isotope Geology, ACTAS, pp. 437–440.
Ripperdan, R.L., 2002. Stratigraphic variation in marine carbonate carbon isotope ratios. In: Valley, J.W., Cole, D.R. (Eds.), Stable Isotope Geochemistry: Reviews in Mineralogy and Geochemistry, 43, pp. 637–662.
Ripperdan, R.L., Miller, J., 1995. Carbon isotope ratios from the Cambrian–Ordovician boundary section at Lawson Cove, Ibex area, Utah. In: Cooper, J.D., Droser, M.L., Finney, S.C. (Eds.), Ordovician Odyssey, Pacific section SEPM, 77, pp. 129–132.
Ripperdan, R.L., Magaritz, M., Nicoll, R.S., Shergold, J.H., 1992. Simultaneous changes in carbon, sea level, and conodont biozones within Cambrian–Ordovician boundary interval at Black Mountain, Australia. Geology 20, 1039–1042.
Ripperdan, R.L., Cooper, J.D., Finney, S.C., 1998. High resolution $\delta^{13}C$ and lithostratigraphic profiles Copenhagen Canyon, Nevada: clues to the behavior of the ocean carbon cycle during the Late Ordovician global crisis. Mineralogical Magazine 62, 1279–1280.
Saltzman, M.R., 2005. Phosphorus, nitrogen, and the redox evolution of the Paleozoic oceans. Geology 33, 573–576.
Saltzman, M.R., Young, S.A., 2005. Long-lived glaciation in the Late Ordovician? Isotopic and sequence-stratigraphic evidence from western Laurentia. Geology 2005 (33), 109–112.
Saltzman, M.R., Runnegar, B., Lohmann, K.C., 1998. Carbon isotope stratigraphy of the Upper Cambrian (Steptoean Stage) sequence of the eastern Great basin: record of a global oceanographic event. Geological Society of America Bulletin 110, 285–297.
Saltzman, M.R., Ripperdan, R.L., Brasier, M.D., Lohmann, K.G., Robison, R.A., Chang, W.T., Pemf, S., Ergaliev, E.K., Runnegar, B., 2000. A global carbon isotope excursion (SPICE) during the Late Cambrian: relation to trilobite extinctions, organic-matter burial and sea level. Palaeogeogeography, Palaeoclimatology, Palaeoecoloy 162, 211–223.
Saltzman, M.R., Bergström, W.H., Huff, W.D., Kolata, D.R., 2003. Conodonts and graptolite Biostratigraphy and the Ordovician (Early Chatfieldian, Middle Caradocian) $\delta^{13}C$ excursion in North America abnd Baltoscandia: implications for the interpretation of the relations between the Millbrig and Kinnekulle K-bentonites. In: Albanesi, G.L., Beresi, M.S., Peralta, S.H. (Eds.), Ordovician from the Andes: INSUGEO, Serie Correlación Geológica, 17, pp. 137–142.
Saltzman, M.R., Cowan, C.A., Runkel, A.C., Runnegar, B., Stewart, M.C., Palmer, A.R., 2004. The Late Cambrian SPICE (δ13C) event and the Sauk II–Sauk III regression: new evidence from Laurentian basins in Utah, Iowa and Newfoundland. Journal of Sedimentary Research 74, 366–377.
Santantonio, M., 1994. Pelagic carbonate platform in the geologic record: their classification, and sedimentary and paleotectonic evolution. American Association of Petroleum Geologists Bulletin 78, 122–141.
Sarmiento, G.N., 1990. Conodontes Ordovicico da Argentina. Treballs Museu Geologia Barcelona 1, 135–161.
Schmitz, B., Bergström, S., Xiaofeng, W., 2010. The middle Darriwilian (Ordovician) $\delta^{13}C$ excursion (MDICE) discovered in the Yangtze Platform succession in China: implications of its first recorded occurrences outside Baltoscandia. Journal of the Geological Society 167, 249–259.
Sial, A.N., Peralta, S., Ferreira, V.P., Toselli, A.J., Aceñolaza, F.G., Parada, M.A., Gaucher, G., Alonso, R.N., Pimentel, M.M., 2008. Upper Cambrian carbonate sequences of the Argentine Precordillera and the Steptoean C-Isotope Positive Excursion (SPICE). Gondwana Research 13, 437–452.
Soufiane, A., Achab, A., 2000. Upper Ordovician and Lower Silurian chitinozoans from central Nevada and Arctic Canada. Review of Palaeobotany and Palynology 113, 165–187.
Stille, P., Chaudhuri, S., Kharaka, Y.K., Clauer, N., 1992. Neodymium, strontium, oxygen and hydrogen isotope compositions of waters in present and past Oceans: a review. In: Chaudhuri, S., Clauer, N. (Eds.), Lecture Notes in Earth Sciences. Springer-Verlag, pp. 389–410.
Tanaka, T., Togashi, S., Kamioka, H., Amakawa, H., Kagami, H., Hamamoto, T., Yuhara, M., Orihashi, Y., Yoneda, S., Shimizu, H., Kunimaru, T., Takahashi, K., Yanagi, T., Nakano, T., Fujimaki, H., Shinjo, R., Asahara, Y., Tanimizu, M., Dragusanu, G., 2000. JNdi1: a neodymium isotope reference in consistency with LaJolla neodymium. Chemical Geology 168, 279–281.
Vaccari, N.E., 1994. Las faunas de trilobites de las sucesiones carbonáticas del Cámbrico y Ordovícico temprano de la Precordillera Septentrional Argentina, doctoral thesis, Universidad Nacional de Córdoba, Argentina, 271 pp.
Young, S.A., Saltzman, M.R., Bergström, S.M., Leslie, S.A., Xu, C., 2008. Paired δ^{13}Ccarb and δ^{13}Corg records of Upper Ordovician (Sandbian–Katian) carbonates in North America and China: implications for paleoceanographic change. Palaeogeography, Palaeoclimatology, Palaeoecology 270, 166–178.